THE SYNTHESIS OF THIN ALUMINA FILM BY PLASMA- ENHANCED ATOMIC LAYER DEPOSITION (PE-ALD)

A THESIS

BY

PARAMAPORN JITSOPAKUL

Presented in Partial Fulfillment of the Requirements for the

Master of Science Degree in Material Science

at Srinakharinwirot University

July 2016

THE SYNTHESIS OF THIN ALUMINA FILM BY PLASMA-ENHANCED ATOMIC LAYER DEPOSITION (PE-ALD)

A THESIS

BY

PARAMAPORN JITSOPAKUL

Presented in Partial Fulfillment of the Requirements for the

Master of Science Degree in Material Science

at Srinakharinwirot University

July 2016

THE SYNTHESIS OF THIN ALUMINA FILM BY PLASMA- ENHANCED ATOMIC LAYER DEPOSITION (PE-ALD)

AN ABSTRACT

BY

PARAMAPORN JITSOPAKUL

Presented in Partial Fulfillment of the Requirements for the

Master of Science Degree in Material Science

at Srinakharinwirot University

July 2016

Paramaporn Jitsopakul. (2016). *The synthesis of thin alumina film by Plasma-Enhanced Atomic Layer Deposition (PE-ALD)*. Thesis, M.S (Material Science). Bangkok: Graduate School, Srinakharinwirot University. Advisor Committee: Asst. Prof. Dr. Duangkhae Bootkul, Dr. Saweat Intarasiri.

Plasma enhanced atomic layer deposition (PE-ALD) is a deposition technique based on sequential self-saturated surface reactions with plasma assisting, leading to the controlled layer-by-layer growth of thin film with atomic layer precision. The advantages of this system provide improvements such as adhesion, smoothness and hardness, as well as enabling uniform deposition of thin film at low substrate temperatures.

This study was an investigation into the physical mechanism of the deposition processing of the Al_2O_3 thin films by PE-ALD and demonstrating low-temperature synthesis of the films grown on Si (1-0-0) substrate. The thin surface oxide films were a result of a reaction between Trimethylaluminum (TMA)-Al $(CH_3)_3$ as an Al source and O_2 plasma as an oxidant, with the argon gas serving as carrier and a purging agent. One cycle of deposition consisted of 2s TMA pulse, 1s argon purge, 4s O_2 pulse and 1s argon purge. The flow rates of TMA and O_2 plasma were 1.0, 7.5 SCCM, and argon purge 1.5 SCCM. Various thin films characterization techniques were applied for the evaluation of properties of the films; e.g. Atomic Force Microscope (AFM), Spectroscopic Ellipsometry (SE), Confocal Raman Spectroscopy, Scanning Electron Microscopes equipped with Energy Dispersive Spectroscopy (SEM/EDS), Transmission electron microscopy (TEM), X-rays diffraction analysis (XRD) and Nano-indentation technique. SE results revealed that the increase in film thickness depended on number of coating cycles and the temperature during deposition; i.e., 3.53 nm, 5.95 nm and 4.59 nm as deposited temperature at 80ºC, 100ºC and 150ºC respectively. While the EDS spectra have shown Al peak, the Raman spectra have revealed vibration of Al-O-Si on samples deposited in an oxygen plasma atmosphere. XRD measurement confirmed that the film in the former condition was AlOx phase. TEM measurement has defined the interface between Al_2O_3 and SiO_2 and indicated the thickness of Al_2O_3 thin film to be about 1.11 nm via HAADF profile maker technique.

Moreover, the first report on the surface nucleation performance of the PE-ALD Al_2O_3 ultra-thin films on crystalline silicon surfaces were briefly tested by Nano-milling technique. Based on these results, the surface chemistry during the plasma enhanced ALD processing of Al_2O_3 thin film was extensively discussed.

การเคลือบฟิล์มบางอลูมินาโดยการตกสะสมชั้นอะตอมแบบพลาสมา

บทคัดย่อ

ของ

ปรมาภรณ์ จิตโสภากุล

เสนอต่อบัณฑิตวิทยาลัย มหาวิทยาลัยศรีนครินทรวิโรฒ เพื่อเป็นส่วนหนึ่งของการศึกษา
ตามหลักสูตรปริญญาวิทยาศาสตรมหาบัณฑิต สาขาวิชาวัสดุศาสตร์
กรกฎาคม 2559

ปรมาภรณ์ จิตโสภากุล. (2559). *การเคลือบฟิล์มบางอลูมินาโดยการตกสะสมชั้นอะตอมแบบพลาสมา*.กรุงเทพฯ: บัณฑิตวิทยาลัย มหาวิทยาลัยศรีนครินทรวิโรฒ. อาจารย์ที่ปรึกษาปริญญานิพนธ์: ผศ. ดร.ดวงแข บุตรกูล, อาจารย์ ดร. เสวต อินทรศิริ.

เทคนิคการตกสะสมชั้นอะตอมแบบพลาสมา อาศัยการควบคุมให้สารอยู่ในสภาวะพลาสมาแล้วตกเคลือบในระดับอะตอมบนพื้นผิวชิ้นงานแบบชั้นต่อชั้นจนได้เป็นฟิล์มบาง ข้อดีของการเคลือบพื้นผิวด้วยวิธีนี้คือการช่วยปรับปรุงคุณสมบัติเชิงกลในด้านต่างๆ ของฟิล์มบาง ได้แก่ สภาพการยึดเกาะ ความเรียบ ความหนาแน่น และความแข็งของฟิล์ม ตลอดจนสามารถเคลือบผิวได้ดีที่อุณหภูมิต่ำ

จุดเด่นของงานวิจัยนี้ คือการอธิบายลักษณะการเกิดฟิล์มบางอลูมินาที่ตกเคลือบบนซิลิกอนเวเฟอร์ชนิดระนาบ (1-0-0) ที่อุณหภูมิต่ำ โดยใช้สารตั้งต้นที่เป็นของเหลว Trimethyl aluminum (TMA, $Al(CH_3)_3$) ซึ่งจะผ่านกระบวนการทำให้เป็นก๊าซและพลาสมา โดยใช้แก๊สอาร์กอนเป็นตัวพาพลาสมาของออกซิเจนมาทำปฏิกิริยากับพลาสมาของ TMA จนเกิดเป็นฟิล์มอลูมินา หนึ่งรอบของการเคลือบนั้นจะประกอบด้วยอัตราการปล่อยของสารในแต่ละตัวดังนี้ 2 วินาที TMA, 1 วินาที อาร์กอน, 4 วินาที ออกซิเจน และ 1 วินาที อาร์กอน

การศึกษาได้ใช้เทคนิคสำหรับตรวจวิเคราะห์ฟิล์มบางหลายรูปแบบ โดยใช้เครื่องมือหลากหลาย ได้แก่ กล้องจุลทรรศน์แรงอะตอม(AFM), เครื่องวัดความหนาฟิล์มบางค่าคงที่เชิงแสงวัสดุ (SE), เครื่องรามานสเปคโตรสโกปี (RAMAN), กล้องจุลทรรศน์อิเล็กตรอนแบบส่องกราดและจุลวิเคราะห์ (SEM/EDX), กล้องจุลทรรศน์อิเล็กตรอนแบบส่องผ่าน (TEM), เครื่องเอกซเรย์ดิฟแฟรกโตมิเตอร์(XRD) และเครื่องวัดความแข็งนาโนอินเด็นเตชัน จากการวิจัยในครั้งนี้ พบว่า ความหนาของฟิล์มบางที่เคลือบนั้น จะขึ้นอยู่กับจำนวนรอบของการเคลือบและอุณหภูมิที่ใช้ในขณะเคลือบ โดยอุณหภูมิ 80, 100 และ 150 องศาเซลเซียส นั้น จะได้ความหนาของฟิล์ม 3.53, 5.95 และ 4.59 นาโนเมตร ตามลำดับ ผลการวิเคราะห์ฟิล์มบางที่เกิดขึ้นในสภาวะที่มีพลาสมาของออกซิเจน ด้วยเทคนิค SEM/EDS พบธาตุอลูมิเนียม สอดคล้องกับการตรวจวัดด้วยเทคนิค RAMAN ที่พบว่าฟิล์มบางที่เกิดขึ้นนั้นมีองค์ประกอบทางเคมีที่ประกอบไปด้วย Al-Si-O นอกจากนี้ผลจาก XRD แสดงให้เห็นความชัดเจนว่ามีการเริ่มต้นการเกิดขึ้นของฟิล์ม AlOx ผลที่ได้นี้ได้รับการยืนยันจาก TEM BF image ซึ่งภาพที่ได้จากเทคนิคดังกล่าวแสดงให้เห็นอย่างชัดเจนว่า มีการแบ่งของฟิล์มในแต่ละชั้น ระหว่างอลูมินาและซิลิกอนออกไซด์ และยังสามารถบอกความหนาของฟิล์มบางอลูมินาได้ว่าอยู่ในราว 1.11 นาโนเมตร สิ่งที่น่าสนใจจากการศึกษาวิจัยในครั้งนี้ คือ สามารถนำเทคนิค TEM ร่วมกับ Nano-milling ศึกษากระบวนการที่เกิดขึ้นของฟิล์มอลูมินาที่อุณหภูมิต่ำตั้งแต่การเกิดขึ้นของนิวเคลียสเล็กๆ ไปจนถึงกลายเป็นฟิล์มบางเคลือบบนซิลิกอนเวเฟอร์ นำไปสู่บทสรุปเชิงลึกของกระบวนการที่เกิดระหว่างการสร้างฟิล์มบางอลูมินา ด้วยเทคนิคการตกสะสมชั้นอะตอมแบบพลาสมา

The thesis titled

"The synthesis of thin alumina film by Plasma - Enhanced Atomic Layer Deposition (PE-ALD)"

By

Paramaporn Jitsopakul

Has been approved by the Graduate School as partial fulfillment of the requirements for the Master of Science degree in Material Science of Srinakharinwirot University.

.....Acting Dean of Graduate School

(Assoc. Prof. Dr. Parin Chaivisuthakura)

July , 2016

Thesis Committee

.....Major-Advisor

(Asst. Prof. Dr. Duangkhae Bootkul)

.....Co- Advisor

(Dr. Saweat Intarasiri)

Oral Defense Committee

.....Chair

(Assoc. Prof. Dr. Dheerawan Boonyawan)

.....Committee

(Asst. Prof. Dr. Duangkhae Bootkul)

.....Committee

(Dr. Saweat Intarasiri)

.....Committee

(Asst. Prof. Dr. Kageeporn Wongpreedee)

Acknowledgements

First of all, I would like to express sincere gratitude to my major- advisor and my co-advisor, Asst. Prof. Dr. Duangkhae Bootkul and Dr. Saweat Intarasiri for all guidance throughout this research and advice as well as for the initiative and possibility to carry out research on this interesting topic.

I am grateful to Ms. Chanitda Prapaipong and Mr. Chanchai Umongno for technical assistances at Plasma and Beam Physics Research Facility (PBP) of Chiang Mai University, Thailand.

I am grateful to Mr. Nattawat Kulrat who XRD measurement for this research was performed at the Department of Physics, Faculty of Science, and Mahidol University, Thailand.

I am also grateful to Mr. Suphakit Pintasiri, Mr. Jirawat Srisung, Ms. Chutima Sedsuttanukul, Mr. Sakthavorn Phongwanitchaya, Ms. Pattarasuda Naknam, and Mr. Natthapon Kongsaeng at Western Digital Thailand for their carried out measurement for this research.

I would like to this opportunity to thank The Western Digital (Thailand) Co., Ltd, and Faculty of Science, Srinakarinwirot University for education financial support.

This work was cooperated among Western Digital Thailand, Plasma and Beam Physics Research Facility (PBP) of Chiang Mai University, Thailand and the Department of General science, Faculty of Science, Srinakharinwirot University, Thailand. The funding by CoE program of Chiang Mai University is acknowledged.

Last I would like to thank my thesis committee member Assoc. Prof. Dr. Dheerawan Boonyawan and Asst. Prof. Dr. Kageeporn Wongpreedee for their time and consideration

Paramaporn Jitsopakul

TABLE OF CONTENTS

TABLE OF CONTENTS (continued)

LIST OF TABLES

LIST OF FIGURES

LIST OF FIGURES (continued)

LIST OF FIGURES (continued)

CHAPTER I

INTRODUCTION

Background

Nowadays, thin films deliver the layer of material which thicknesses ranging from few angstroms to tens of micrometer, demanding of several industries and applications. The thin film technology trends to down scale and miniaturization into atomic-level. Atomic layer deposition (ALD) is one of a promising method to meet the trends. ALD is a vapor-phase deposition technique modifying from chemical vapor deposition technique (CVD). This method is based on sequence of alternating pulses of gaseous chemical precursors into the chamber, follow by separation with inert gases, which react with the substrate and saturate the film growth. It could be possible for a variety of materials formation from pure metal to oxide, nitrites, and polymers to deposit various substrates materials for various industry requirements. Moreover, the film structure formed by ALD appears to be unique feature over other techniques because of the excellence film quality, the good step coverage, the controlled stoichiometry of thickness at angstrom level, and the pin hole free [1, 2].

Plasma Enhance Atomic Layer Deposition (PE-ALD) provides several benefits over the conventional ALD technique by introducing the plasma to support the chemical reactions in the chamber. The successful key of the PE-ALD during the thin film deposition relates to the reactive species generated in the gas-phase. Typically, the plasma supplies a low heat flux to the surface and at the same time, additional energy could be provided to the depositions surface due to ion bombardment [3]. The technique provides excess energy for the adsorbed species, thus increasing the surface mobility, resulting in the increasing of film density, and reducing interface structure, which affect the density between film materials and self-substrate.

Moreover, the ability to synthesize at low temperature is suitable for polymeric materials deposition for biological applications. The advance industry applications of PE-ALD are coating protection of a magnetic recording heads for hard disk drive, protective coat reaction of micro-electro mechanical systems, gate insulators, capacitors, barrier, solar cells, optical device, electro–luminescent devices, and thin film transistor [4].

Alumina (Al_2O_3) film is an important protection layer material due to its excellent dielectric property, high hardness, good adhesion to many surfaces, thermal and chemical stability. Al_2O_3 is metastable polymorphs exiting in many forms such as $\alpha, \gamma, \kappa, \theta$ - Al_2O_3.

These difference phases appear to hold different properties. α- Al_2O_3 film has been mainly select for high temperature applications such as covering steel and cutting tools due to its high thermal resistance and excellent mechanical properties. κ- Al_2O_3 film was able to enhance wear resistance for high temperature applications, due to its high hardness, as an alternative to α - Al_2O_3 [5]. γ- Al_2O_3 film with low surface energy property was used in catalysis due to its large surface area [6].

This research aims to investigate the Al_2O_3 thin film property deposited with PE-ALD technique on Si (1-0-0) wafer, mainly for mechanical properties applications. The PE-ALD system was self-constructed by the Plasma and Beam Physics Research Facilities (PBP) of Chiang Mai University, Thailand. The Al_2O_3 thin films were deposited using Trimethyl aluminum (TMA, Al $(CH_3)_3$) as a precursor and O_2 as an oxidizing agent on Si (1-0-0). The film properties were investigated by numerous techniques in terms of surface characteristics, thin film structure and mechanical properties of the films, i.e. Atomic Force Microscopy (AFM), Spectroscopic Ellipsometry (SE), Raman Spectroscopy, X-ray diffraction(XRD),Scanning electron Microscope(SEM/EDX), Transmission Electron Microscopy (TEM), X-ray Photoelectron Spectroscopy(XPS), and Nano-indentation measurement.

Objectives of the research

The thesis deals with synthesizing of Al_2O_3 thin film on Si wafer (1-0-0) substrate by PE-ALD technique under low temperature at 80°C, 100°C, and 150° with controlling coating cycles 400, 800 cycles and controlling plasma condition during deposition process. The specific objectives of the thesis are follow;

1. To investigated the synthesizing of Al_2O_3 thin film deposition with PE-ALD at low temperature.
2. To investigate the mechanical properties and the characteristics of the thin film after deposition of each condition.
3. To draw up the physical mechanism behind the film formation by PE-ALD.

Significance of the research

This thesis described several significant technological impacts as follow:

1. The process of Plasma Enhance Atomic Layer Deposition (PE-ALD) for synthesizing the ultra-thin alumina film under low temperature (less than 300^{o} C). This technique yield excellent thin film properties, higher film density, and lower impurity.

2. Surface roughness analysis using Bruker's Dimension Icon with tapping mode. The resolution image is in sub-nano level and low distortion.

3. Thin film thickness measurement using M-2000 Ellipsometer (J.A Woollam Co. Ellipsometry Solution) that applied RCE (Rotating Compensator Ellipsometer) technology to achieve high accuracy and precision measurement of ultra-thin films of thickness < 10nm with no sample preparing.

4. Morphology and elements analysis using SEM (SE, EDS mode) (Zeiss Merlin). This model combines fast analytics, high resolution imaging using advanced detection modes, acceleration voltage of 0.02 – 30 kV and characteristic X-rays of 1-3 μm analysis depth.

5. Molecular species of thin film analysis using Raman Spectroscopy JOBIN YVON HORIBA spectrometer HORIBA (T64000) with confocal techniques. It is possible to analyze individual particles or layers with dimensions down to 1 μm or below for a true confocal design.

6. Chemical analysis using XPS (AXIS Ultra DLD) to determine chemical composition of deposited thin film with no effects to the sample surface. The minimum thickness is able to measure to about 10 nm.

7. Phase composition of thin film analysis using XRD (Bruker D8), with Grazing Incidence X-ray Diffraction (GIXRD) mode. X-ray diffraction is able to measure thin films of 1-1000 nm thickness. The diffraction can be made surface sensitive.

8. Interface and thin film properties observing using TEM (FEI Osiris with super X-EDS Bruker Nano GmbH), including cleaning thin film surface with Nano milling for eliminating contamination or some residue on thin film surface to enhance the benefit of HAADF scanning elements detection.

9. Nano-indentation measurement with Berkovich tip, for measuring mechanical properties of materials in term of hardness and elastic modulus from micro- to Nano-scale.

Scope of the research

1. Set up optimum condition of PE – ALD for deposition of Al_2O_3 thin film on Si – wafer substrate.

2. Synthesis Al_2O_3 thin film by controlling coating cycle 400, 800 cycles, with and without plasma assisting during deposition and controlling temperature to 80°C, 100ºC and 150ºC during deposition.

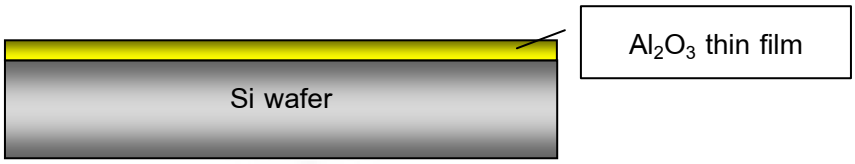

Figture 1 The schematic of Al_2O_3 thin film on silicon wafer

1. The flowchart of thin film synthesis and characterization is illustrated below.

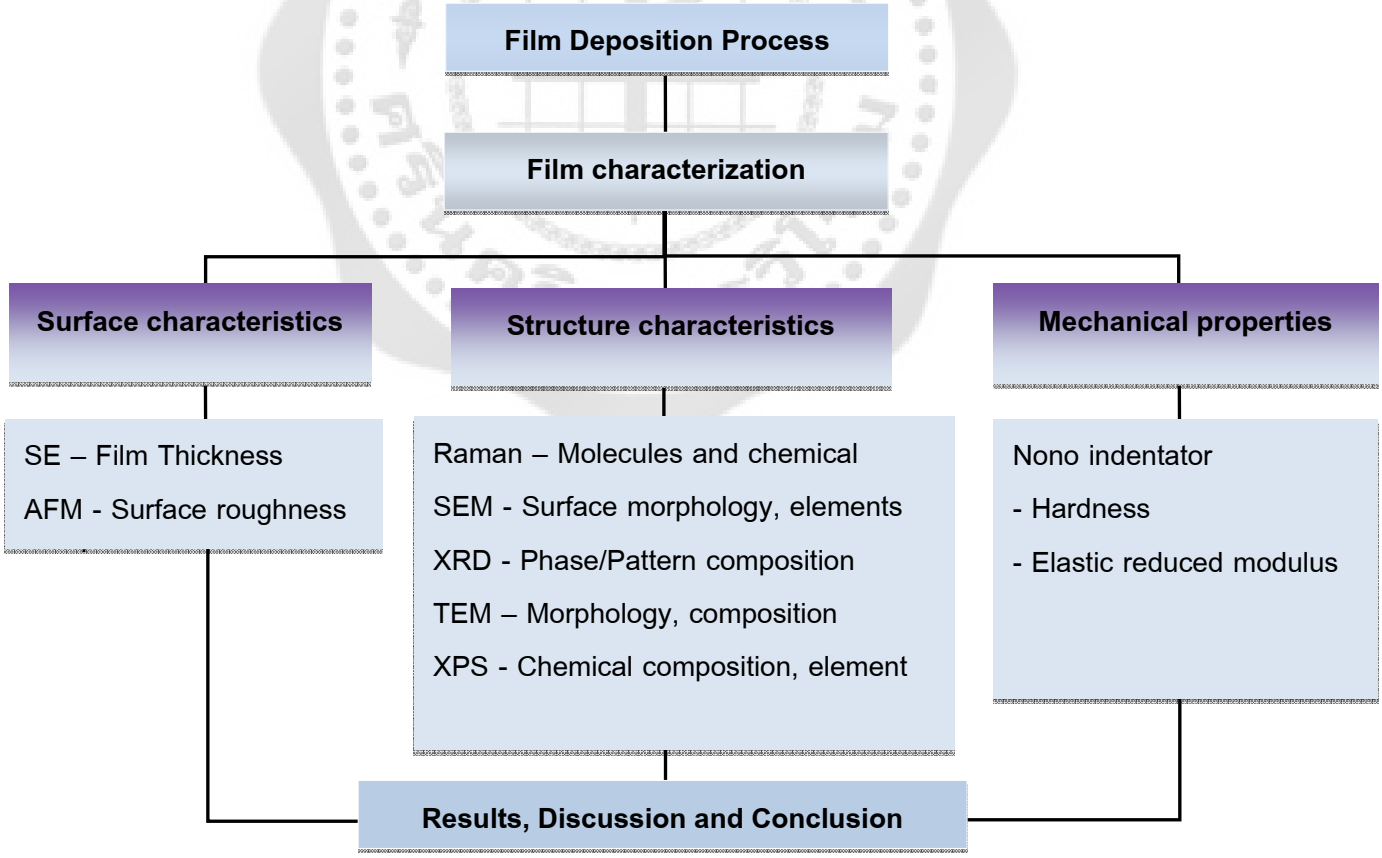

Figture 2 Flowchart of thin film synthesis and characterization.

Framework

Synthesizing Al_2O_3 thin film using Plasma Enhance Atomic Layer Deposition (PE-ALD) technique, by comparing coating cycle and plasma control condition for with and without plasma assisting, and thin film characterization.

Research Hypotheses

1. Al_2O_3 thin film could be able to deposit with PE-ALD at low temperature.
2. Al_2O_3 thin films have excellence mechanical properties.

Definition of terms

1. **Atomic Layer Deposition (ALD)** is thin film deposition technique. It is modified from chemical vapor deposition technique (CVD). This technique based on sequence use of self-terminating growth gas-solid reaction.

2. **Plasma Enhance Atomic Layer Deposition (PE-ALD)** is thin film deposition technique by inducing plasma for energy-enhanced to the synthesis of ultra-thin films with Angstromº level. This technique provides several benefits over the conventional ALD, thus improving material properties.

3. **Thin film** is a layer of material with thickness having varied from a few angstroms to 10 micrometer.

4. **Growth per Cycle (GPC)** is described the repeat layer by layer to increase amount of material to the surface to meet prefer thickness.

5.**ALD window** is described the temperature range of growth per cycle (GPC) in ALD process, requirement of self-terminating reaction by the precursor to adsorb to the surface which is mainly thermally driven.

6.**Cluster** is a small group of atoms or molecules or a number of things of the same kind, growing or held together.

7. **Amorphous** is having no definite form.

8. **Conformity** defines how uniform film thickness is reproduced over the topography of a structured substrate.

9. **Homogeneity** is used to describe uniformity of film properties across substrate and film thickness.

10. **Interface** is a surface that forms the boundary between two bodies, liquids, or chemical phases.

11. **Nucleation** is a formation of stable small particles (nuclei) of the new phase. Nuclei are often formed at grain boundaries and other defects.

12. **Surface roughness** or shortly roughness is a component of surface texture. It is typically calculated as arithmetic average, RA, or root mean square, RMS, of vertical deviation from reference plane.

CHAPTER II

REVIEW OF THE LITERATURES

This chapter reviews basic knowledge and advance literatures relevance to the thesis within the following items.

1. Structure and properties of Alumina (Al_2O_3)
2. Thin film techniques
3. Atomic layer deposition (ALD)
4. Plasma Enhance Atomic layer deposition (PE-ALD) system
5. Characterization tools for thin film
6. Physical mechanism reviewed

1. Structure and properties of Alumina (Al_2O_3)

Alumina is a ceramic material with common name as aluminum oxide (Al_2O_3). It is an oxide form of the metal aluminum and occurs in nature as minerals corundum (Al_2O_3), diaspore ($Al_2O_3 \cdot H_2O$), gibbsite ($Al_2O_3 \cdot 3H_2O$) and basic aluminum oxide as boehmite (AlO(OH)). The importance source of aluminum is bauxite, the clay like rock minerals, which contains alumina, oxygen, and water. Each oxide form contains different alumina content leading to possess different mechanical and physical properties [5, 7], as shown in Table 1.

Table 1 Properties of alumina hydrates [7].

Designation	Gibbsite	Boehmite	Diaspore
Alumina content (%)	65.4%	85%	85%
System crystalline	Monoclinic	Orthorhombic	Orthorhombic
Hardness (GPa)	2.5-3.5	3.5-4.0	6.5-7.0
Product of dehydration	X-Al_2O_3	Y- Al_2O_3	Z- Al_2O_3
Density (g/cm^2)	2.42	3.01	3.44

Al_2O_3 structure can be divided to two categories depending on an arrangement of oxygen anion, i.e. face centered cubic (FCC) and hexagonal close packed (HCP). The structure of Al_2O_3 based on FCC packing including γ, δ, η, and θ, while the structure of Al_2O_3 based on HCP packing are represented by α, κ, and χ phases [8], as shown in Table 2.

Table 2 The Structures and properties of alumina polymorphs [9], [10]

Phase	Structural arrangement of oxygen	Density(g/cm^2)	Young's modulus (GPa)	Melting point (°C)
γ	FCC	3.65-3.67	253-275	γ ⟶ δ: 700-800
κ	HCP	3.98	362	-
θ	FCC	3.60-3.65	-	θ ⟶: α: 1050
α	HCP	3.96-3.99	409-441	2051
δ	FCC	3.60-3.65	-	-

There are many forms for alumina phase, but only corundum (α–Al_2O_3) is the thermodynamically stable forms at all temperatures up to its melting point. Material property of phase is summarized in Table 3. The others phases are known as metastable phase and can be transformed to α-Al_2O_3 by heat treatment, for example aluminum hydroxides or aluminum salt [11]. Typically α-Al_2O_3 transformation takes place at above 1,000°C, while metastable phases are formed at temperature lower than 1000°C. This is because the metastable phases are surface energy stabilization at the initial growth stage. The sequence transformation of alumina and aluminum hydroxides depend on the starting material, its coarseness and crystallinity, heating rate, the amount of water vapor in the atmosphere and the impurities presented, as shown in Figure 3.

Table 3 Material properties of Aluminum oxide (α-Al_2O_3) (99.5%) [8].

Material properties	Aluminum Oxide (Al_2O_3)
Hardness	13-15 GPa
Tensile Strength	260-300 MP
Thermal conductivity	35 W/m-K @R.T.
Young's Modulus	393 GPa
Fracture Toughness	4.5 $MPa.m^{1}/_{2}$
Dielectric Constant	9.6 1HHz@ R.T.
Density	3.89($lb./ft^3$)
Refractive index	1.76
Band gap	8.8 eV

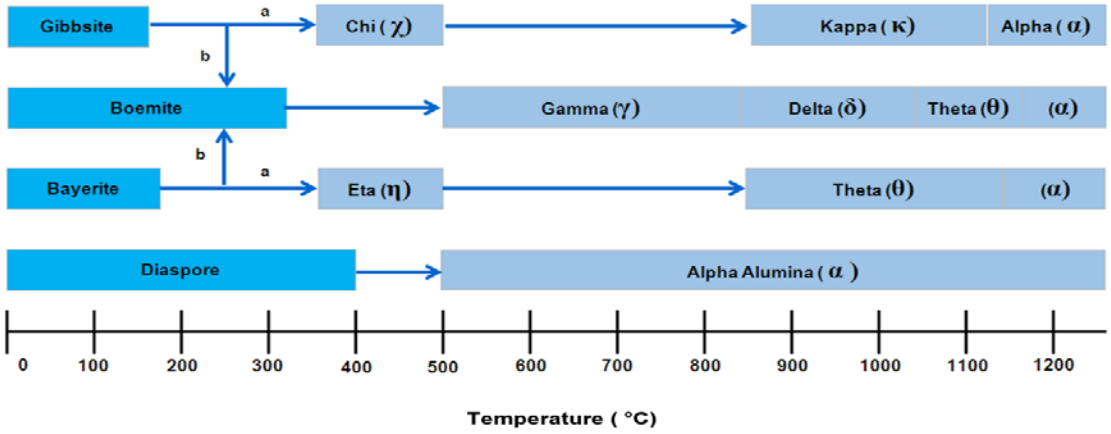

Figure 3 Structural transformation of alumina and aluminum hydroxides [11].

The alumina film also exists in different phases depending on the alumina purity and there mechanical and physical properties are varied significantly [5]. α-Al_2O_3 film was mainly selected for high temperature applications such as covering steel and cutting tools due to its high thermal resistance and excellent mechanical properties. κ-Al_2O_3 film was able to enhance wear resistance for high temperature applications, due to its high hardness, as an alternative to α-Al_2O_3 [4, 5]. γ-Al_2O_3 film with low surface energy property was used in catalysis due to its large surface area [5, 6, and 12]. The property and application of alumina film can be summarized in Table 4.

Table 4 Summarization of Al_2O_3 film properties and its applications.

Material properties	Applications
Hardness	Cutting tools /Hard coating, to improve wear resistance of surface material properties and its applications.
High refractive index	Optical coating /Solar panels, to improve refractive index of film.
Low electrical conductivity	Electronic devise pinhole-free
High thermal conductivity	Coatings semiconductor material
High band gab	Dielectric and insulator material
Antistatic coating	Plasma display, LCD, Touch panels

2. Thin film techniques

2.1 Thin film growth and nucleation

At initial thin film growth state, the surface energies are importance, i.e. the material surface covering with various types of adsorbed species. The substrate need to have suitable adsorption sites to initiate the growth during the first cycles. Normally thin film growth process depends on deposition conditions such as the substrate temperature and the contents/kinetic energies of the deposition flux [13, 14]. The atomic process occurs during thin film growth is shown in Figure 4.

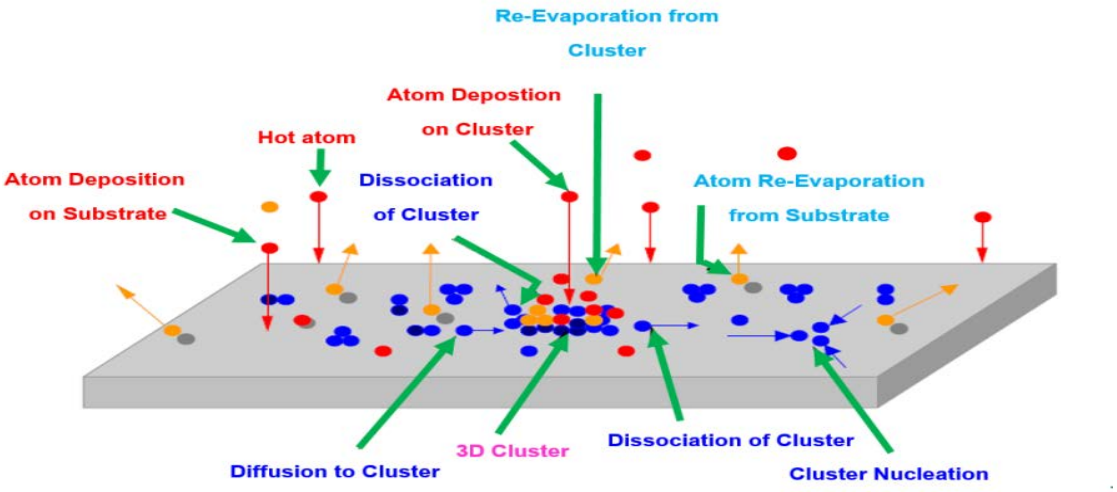

Figure 4 Schematic of atomic process occurs during thin film growth [14].

Nucleation is the formation of stable few particles or nuclei of the new phase concerning with thermodynamics relating to the energetics of forming a single stable, occurring during the early stage of phase change. Nucleation can be classified to two types; the first type is homogeneous nucleation occurring when nuclei uniform spread across substrate and through film thickness; the second type is heterogeneous, nuclei form at structure in homogeneities likes impurities, grain boundaries [13]. Thin film growth mode can be classified to three modes depending on the materials arrangement on the substrate surface during film deposition process. The factors concerning are temperature, step-edge barriers, deposition rate and energetic bombardment [13] as shown schematically in Figure 5.

(a) (b) (c)

Figure 5 Thin film growth mode; (a) Volmer-Weber; (b) Frank-van-der-Merwe; (c) Shranski-Krastanov [13].

(a) Volker-Weber (Islands structure), island growth occurs when the smallest stable clusters nucleate on the substrate and grow in three dimensions to form islands. This happens when atoms or molecules in the films are more strongly bound to each other than to the substrate. .

(b) Frank-van-der-Merwe (Uniform film), in this growth mode the atoms are more strongly bound to the substrate than to each other. The first complete monolayer is then covered with a somewhat less tightly bound second layer. Providing the decrease in bonding energy is continuous toward the bulk-crystal value, the layer growth mode is sustained.

(c) Stranski–Krastanov (Islands or uniform film layer), in this growth mode the adsorbate-surface interactions are stronger than adsorbate-adsorbate interactions.

2.2 Alumina thin film techniques

Al_2O_3 phase formation depends on temperature during deposition which also affected to the differentce in its property. Normally, amorphous Al_2O_3 is dominant at low temperature, while crystalline κ- and $\alpha-$ phases dominant at high temperature [15]. As the growth temperature is increased, Al_2O_3 phase trends to evolution from amorphous (350-550°C) to crystalline (beyond 550°C), crystalline ones consisting of κ- and γ- Al_2O_3 (750-950 °C), and crystalline κ-Al_2O_3 films at 950 °C [5]. Many techniques can be applied to growth α-Al_2O_3 such as grown by chemical vapor deposition (CVD). This technique is the reacting volatile gas or vapor precursor passing over a heated substrate surface which shall be formed and let into the reaction chamber.

Film is obtained via chemical reaction on substrate. This technique provides high quality films and able for effectively homogeneous coatings with structural uniformity on substrate having complex geometries. But the limitation of this method is requiring high temperature and low pressures, and might be leading to a problem when the substrate cooling down due to the different thermal expansion coefficients of film and substrate [13, 15]. CVD technique was used to growth film for cutting tools application by deposition at high substrate temperature of 1100 °C [15].

The physical vapor deposition (PVD) is also one of a technique applying for α-Al_2O_3 growth. PVD is the technique utilizing physical means to transfer atoms from target to substrate by evaporation or sputtering or ion plating [13]. This technique is able to deposit film at lower substrate temperature than CVD, and it can apply for deposition of a wide range of substrates. The properties of film depend on microstructure, crystal phase, film composition and the thickness which can be controlled during the deposition [16]. The synthesis methods and growth temperature for alumina polymorphs are shown in Figure 6 [9]

Figure 6 The synthesis methods and growth temperatures for alumina polymorphs [9].

Note; T-CVD = Thermal CVD, PE-CVD = Plasma Enhance chemical vapor deposition, MS = Magnetron sputtering, HPPMS = High power pulsed magnetron sputtering, ARC = Cathodic Arc.

However, both CVD and PVD still have limitation. The CVD technique requires high substrate temperatures (from 1,000°C) to provide the good film and to form species with the energy enough for Al_2O_3 phase formation. These high deposition temperatures may cause

the thermal stress, leading to poor adhesion and inducing crack formations [9]. PVD technique requires lower substrate temperature than CVD technique but obtaining the lower film quality.

Table 5 presents the comparison of thin film techniques in term of the film properties, such as thickness, step coverage, and temperature during deposition. Atomic layer deposition (ALD) has more benefits than the other techniques in order to fulfill the future requirement of miniaturization progressing in nanometer scale level of industries. This technique suitable for supporting thin film application in term of thin film quality and low substrate temperature during deposition which applicable for many industrials, such as electronic components, electronic displays, magnetics films for data storage, optical coating, optical data storage devices, antistatic coatings and hard surface coating [2].

Table 5 Comparison of deposition techniques for thin film growth [17].

Attribute	CVD	ALD	PLD	S	E
Thickness uniformity	Good	Good	Fair	Good	Poor
Film density	Good	Good	Good	Good	Poor
Step coverage	Vary	Good	Poor	Poor	Poor
Interface quality	Vary	Good	Vary	Poor	Good
Low temperature	Vary	Good	Good	Poor	Good
Deposition Rate	Good	Fair	Good	Good	Good
Industrial Applications	Good	Good	Poor	Good	Good

Note: Chemical Vapor Deposition (CVD), Atomic Layer deposition (ALD), Physical Vapor Deposition (PVD), Sputtering (S, Evaporation (E), and Pulsed Laser Deposition (PLD) [17]

3. Atomic Layer Deposition (ALD)

3.1 ALD Principle Processing

Atomic layer deposition (ALD) is a promising thin film deposition technique. It is modified from chemical vapor deposition technique (CVD). This technique based on sequence use of self-terminating growth gas-solid reaction. The precursor pulsed into

chamber one at the time and separated by inert gas. The reactions are saturated and the film growth is thereby self-limiting. The film thickness is determined by the number of cycles which fully completed all stages before start the next step [18]. The advantages of ALD comparing to other deposition methods are feature of good film quality, excellent high aspect ratio nanostructure, step coverage, controlling stoichiometry of thin film, pin hole free and controlling thickness of films to atomic-level. The technique can achieve to the industrial requirement and applicable for many functions to meet the current trend of down scaling and miniaturization in Nano-scale level [1]. The basic of ALD cycles consist of 4 steps [1] as shown in Figure 7.

(a) The first precursor (TMA) is pulsed into the reaction chamber, then the chemical species absorbed on the substrate surface until the surface completely coverage and saturated.

(b) Purge inert gas with argon to remove the unreacted precursor, by product (CH_4) and contamination out of the chamber.

(c) The second precursor (O_2 plasma) is pulsed into the chamber and reaction with absorbed on surface until saturated.

(d) Purge with gas flow or evacuation to remove the unreacted precursor and by product (CH_4) and contamination out of the chamber.

Figure 7 Schematic representation of thermal ALD cycle (with H_2O dosing) and plasma-assisted ALD cycle (with O_2 plasma exposure) [1].

ALD cycle is repeated layer by layer to increase amount of material to sample surface until achieve prefer surface thickness, knowing as growth per cycle (GPC). The chemistry occurring during the initial growth of the ALD process starts with nucleation, once nuclei are formed on the substrate and uniform distributed then island rapid growth, thus increasing a surface area. The next stage involves merging of islands or coalescence, the surface area is decreased achieving a stable value of growth rate. Secondary nucleation could occur at a later stage, which increases the surface area again for the next cycle [18]. ALD growth rate depends on materials, precursor, and ALD tool operations. The schematic of the process is shown in Figure 8.

Figure 8 Schematic of the chemistry occurs during the initial growth in an ALD process [18].

The ALD window concept can describe the temperature range of GPC in ALD. These are four steps of the GPC which may depend on temperature in the ALD window as shown in Figure 9. Condensation and decomposition of precursor lead to increase growth per cycle while incomplete reaction and desorption lead to decreased growth per cycle [2]. The ALD-window is a good tool for investigation the temperature window of the precursors. During deposition at low temperature, films are almost amorphous while at high temperature films become crystalline. In additional, the reaction and mass transfer kinetic also increase with temperature in which higher temperature more efficiency for diffusion and mobility of atom and molecules, thus influence to the crystallinity of films [18].

Figure 9 Schematic of possible behavior for ALD growth per cycle versus temperature showing the ALD window [2].

The ALD window is the growth rate constant correlation with the temperature during deposition. In the growth process, it is almost one monolayer per cycle as reported by Gieraltowska [19]. He studied the ALD deposition of dielectric oxides for MIS structures. The results have shown ALD window for Al_2O_3 between 180°C to 200°C giving the growth rate of 1.0 Å per cycle as shown in Figure 10.

Figure 10 The growth rate of the Al_2O_3 films as a function of deposition temperature. ALD window is in the range of temperatures 180°C-200°C [19].

3.2 Surface Chemistry of ALD

The process of ALD is based on sequential self-terminating of gas–solid reactions. The adsorption can be divided in two general classes based on strength of interaction between the adsorbing molecule and the solid surface [13, 19] as shown in Figure 11. This diagram displays difference types of monolayer of ALD; (a) a chemisorbed monolayer; (b) a physisorbed monolayer; and (c) a monolayer of the ALD-grown material [19, 20].

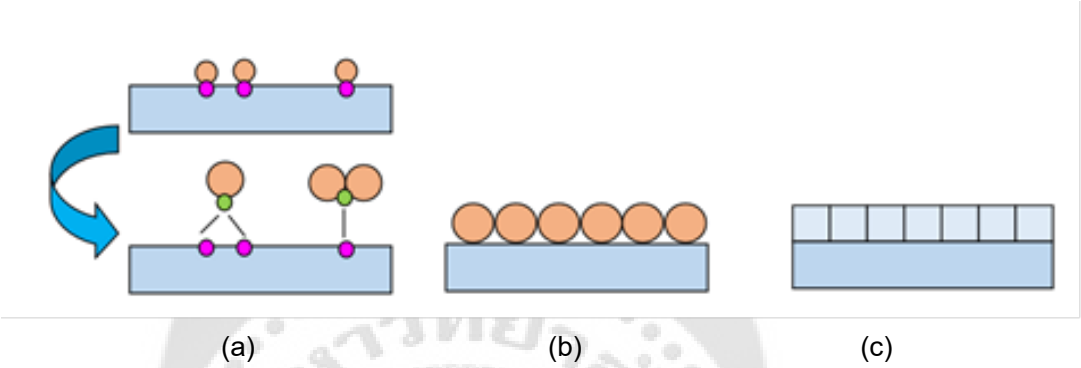

(a) (b) (c)

Figure 11 Different types of monolayers relevant to ALD; (a) a chemisorbed monolayer; (b) a physisorbed monolayer; and (c) a monolayer of the ALD-grown material [19, 20].

As for nature of ALD process, it is necessary to have an irreversible adsorption on the substrate. This means that each precursor must be capable to form chemical bonds through chemisorption onto the chemisorbed species of the previous precursor.

Chemisorption reactions are heterogeneous gas-solid reactions. Chemisorption involves the formation of chemical bonds, as opposed to Physisorption. They are also called reaction by the force of attraction in the chemical bonding. It is irreversible with high heat of adsorption. For Physisorption, the molecules are attracted by van der Waals forces. The binding energy depends on the polarizability and force between surface. It is reversible with low heat of adsorption [20].

The ALD model system prefers for reaction of Al_2O_3 [2, 21]. In this technique Al_2O_3 film usually using trimethylaluminum [Al $(CH_3)_3$] (TMA) as first precursor. The Al_2O_3 ALD growth during exposure to TMA and H_2O is very high efficient and self-limiting. In the first ALD half-cycle, the Al $(CH_3)_3$ precursor reacts through ligand exchanging with the surface hydroxyls under formation of methane and O–Al bonds. This reaction is very efficient due to the formation of the strong O–Al bond. The latter becomes more important at low substrate temperatures because of the high density of surface OH groups. The surface chemistry

during the first half-cycle is similar for both plasma and thermal ALD, and can be describe by

$$Al\text{-}OH^* + Al(CH_3)_3\ (g) \longrightarrow AlO\text{-}Al(CH_3)_2)^* + CH_4 \quad (1)$$

During the second half-cycle, the surface is changes from methyl-terminated to hydroxyl-terminated. For thermal ALD, methane is produce during the second half-cycle via (2)

$$AlO\text{-}AlCH_3^* + H_2O\ (g) \longrightarrow AlOAl\text{-}OH^* + CH_4\ (g) \quad (2)$$

The overall reaction for Al_2O_3 ALD is

$$2Al(CH_3)_3 + 3H_2O \longrightarrow Al_2O_3 + 3CH_4 \ , \Delta H = -376\ kcal \quad (3)$$

For plasma ALD, the reactions can be summarize by

$$AlO\text{-}AlCH_3^* + 4O\ (g) \longrightarrow AlOAl\text{-}OH^* + H_2O\ (g)\ CO_x\ (g) \quad (4)$$

3.3 ALD Precursor

The precursor is one factor of ALD process. In general, precursor can be in the form of gas, either liquid or solid. The main requirements for a good ALD precursor can listed as follows. ALD precursors are volatility, thermal stable (gas, solid or liquid), rapid reaction on surface, aggressive, complete reactions, non-toxic, environment friendly, no self-decomposition, no etching of the film or substrate materials, sufficient purity, un-reactive volatile by-products, easy to synthesis. Normally precursor can be classified to two cases, such as metal precursor (halides, alkyl compounds, and alkoxides) and non-metal precursors. The latter is usually hydrides (H_2O, H_2S, NH_3 and AsH_3), oxygen source H_2O, O_3, O_2, N_2O, H_2O_2, oxygen radicals, and metal alkoxides [20, 22].

4. Plasma Enhance Atomic Layer Deposition (PE-ALD)

Plasma Enhance Atomic layer deposition (PE- ALD) provides more benefits than thermal ALD by inducing plasma source to support the chemical reactions leading to improving material properties, such as higher film density, lower impurity levels, better control of film composition and microstructure, increasing growth rates per cycle (GPC), lower temperature processing, and available for various substrate materials [3].

4.1 The basic and properties of plasma

The plasma is free electric charged or charged particles with different concentrations of charge state. Most of plasma creates by electrical fields leading to acceleration and heating of the electrons. The reactant gas is dissociated and excited through electron impact collisions [4]. Plasma consists of collection of electrons, ions, and neutral atomic and molecular species [13]. Plasma can induce surface reactions when arriving at the deposition or reactor surfaces. The energetic particle bombardment of the growing film surface plays a significant role during the film growth processing, mostly effected by the substrate temperature and the kinetic energy of the plasma species. If a solid is placed in a glow discharge, both ions and electrons would hit the surface. Nevertheless, electrons can move significantly faster than ions.

In PE-ALD, plasma is overspread gas to produce radical. The proximity of plasma discharging to the substrate resulting in large flux of radical is the major advantage of PE-ALD. The bombardment or energy from plasma may increases the energy to absorbed species and increases the surface mobility allowing reaction in films formation. The effect of plasma may result in surface damage and the close proximity of the plasma discharging may result in dissociation of possible reaction by-products or adsorbed precursors and thereby leading to contamination [4, 13]. The key of the plasma steps during synthesis of thin film by PE-ALD [4] are:

(a) The reactive species are creating in the gas-phase.

(b) Typically, the plasma supplies a relatively low heat flux to the surface.

(c) Through ion bombardment, additional energy can be provided to the deposition surface.

Typical plasma using during PE-ALD deposition is originated from O_2, N_2 and H_2 or combinations reactant gases allowing the deposition of metal oxides, metal nitrides, and metal films.

4.2 The System of Plasma Enhance Atomic Layer Deposition (PE-ALD)

In this thesis, films deposition were performed using Plasma-Enhanced Atomic Layer Deposition (PE-ALD) system developed by the Plasma and Beam physics Research Facilities (PBP), Chiang Mai University, Thailand [23] as shown in Figure 12.

Figure 12 Plasma-Enhanced Atomic Layer Deposition (PE-ALD) systems of PBP, Chiang Mai University.

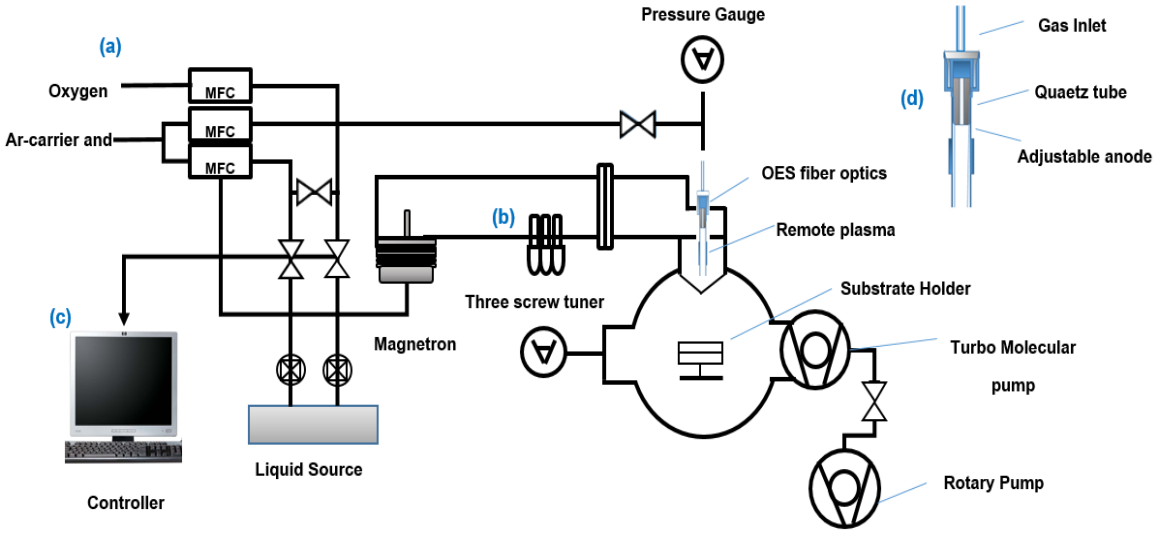

Figure 13 Schematic diagram of the PE –ALD system.

This system consists of three sub systems; (a) Gas feeder; (b) The microwave remote plasma and multicusp chamber; and (c) The computer controller; and (d) details of the plasma source tube [23].

The system of PE-ALD consists of three sub-systems, including precursor feeder system, microwave remote plasma and control system as shown in Figure 13.

(a) The precursor of feeder system. This system consists of three mass flow controllers that supply three functions of gas flow phase. The first function is argon as purging gas to chamber including carrier gas of Trimethyl aluminum (TMA, Al $(CH_3)_3$) which is the first precursor to transition phase from liquid phase to vapor phase of precursor. The last function uses oxygen for the second precursor to generate plasma during deposition.

(b) Microwave remote plasma systems and multicusp chamber and sub-system. This system consists of plasma source and microwave source. Microwave power generates dense plasma in source tube that is mount on top of chamber and diffuses to reaction chamber. In this system additional multicusp (or magnetic multipole) improves plasma density by reaction of magnetically line wall to protect the discharge anode and maintain large volume of discharge leading to increasing plasma density.

(c) The main system of PE-ALD is the Controller system. The system connects and synchronizes all mass flow allowing for designing the number of cycle and purging range of precursor (TMA, O_2, and Argon-purge) during ALD deposition

5. Characterization tools for thin film

5.1 Atomic Force Microscopy (AFM)

AFM is a technique based on interaction force between sample surface and a sharp tip that mounted on a flexible cantilever when tip close to surface, and measuring attractive or repulsive forces between a tip and the sample with van der Waals forces (VdW). AFM provides topographic image of a surface with atomic resolution in all three dimensions as shown in Figure 14. The magnitude of the deflection depends on the distance between the tip and the sample.

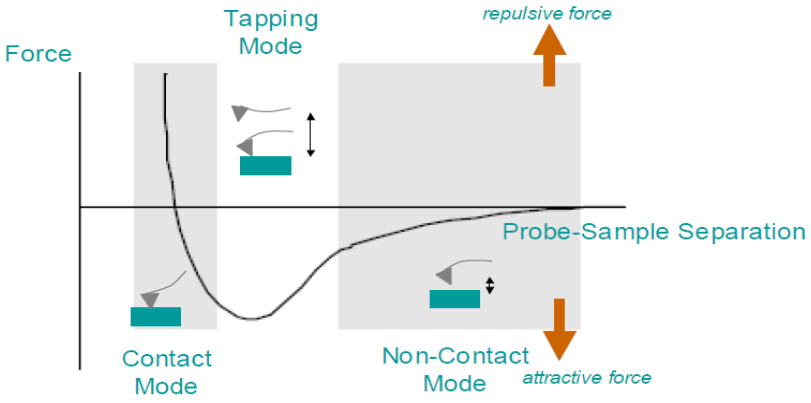

Figure 14 Plot of force as a function of probe-sample separation [24]

There are three different AFM modes used for topography imaging, which are non-contact mode, contact mode, and tapping mode. For this research, tapping mode is preferred for characterization the surface roughness of deposited thin film.

For tapping mode, the tip oscillates near its resonance frequency and it intermittently interacts with the sample surface. Constant oscillation amplitude is use as a feedback mechanism to maintain a constant tip-sample interaction. This mode is high resolution without inducing destructive frictional forces, thus the very soft and fragile samples can be image successfully.

Surface roughness is a component of surface texture and it can be characterized by several parameters and functions, such as height parameters, wavelength parameters, and spacing and hybrid parameters. All these parameters based on two-dimensional standards that are extend to three dimensions, giving information about statistical average values, shape of the histogram heights and other extreme properties. The roughness parameters are estimate by analyzing the topography scans of the sample's surface [25]. This research used profile parameters of Ra and Rq to represent the surface roughness of the deposition thin film in comparison with Si virgin substrate.

Average roughness (Ra) is the area between the roughness profiles. It is useful for detecting general variations in overall profile of height characteristic and for monitoring an established manufacturing process.

$$Ra = \frac{1}{l}\int_0^l \left| z(x) \right| dx \qquad (5)$$

Root mean square roughness (Rq) is measured the overall roughness of a surface by taking a number of surface irregularity readings and then calculating the square root of the mean of squares from those readings. It is considered more sensitive than the average roughness for large deviations from the mean line/plane. It also describes the finish of optical surfaces. It represents the standard deviation of the profile heights. Higher RMS numbers indicate rougher surfaces, while lower numbers indicate smoother surfaces. Rq provides information $\cong$ 1.1 x Ra.

(6)

$$Rq = \sqrt{\frac{1}{l}\int_0^l z^2(x)\,dx}$$

Cimalla et al. [26] reported on surface roughness of Al_2O_3 thin film after deposition with PA-ALD, with thickness 40 nm; Rq was 0.2 nm after coating and increased to 0.5 nm after annealing in N_2 at 900º C as seen in Figure 15.

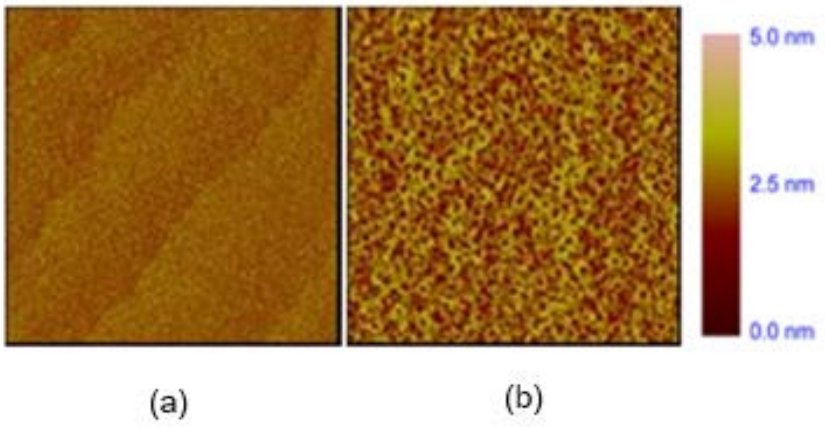

Figure 15 Surface roughness of Al_2O_3 thin film after deposition with PA-ALD.
(a) Surface roughness as deposited, (b) Surface roughness after annealing [26]

5.2 Ellipsometry Spectroscopy (SE)

Ellipsometry Spectroscopy (SE) is a non-destructive and light optical analysis technique that can provide both thin film metrology and optical technique. This technique is measured the state of polarization of the light that reflect from sample surface. It can analyze both single and multi-layer samples with accurate measurement of ultra-thin films of thickness < 10nm with no sample preparation. The schematic of (SE) is shown in Figure 16.

Figure 16 Schematic of an Ellipsometry system and light reflection model.

The relation of the basic equation in Ellipsometry is giving by the complex ratio ρ of the two reflection coefficients.

$$\rho = \frac{R_P}{R_S} = \tan(\psi)e^{i\Delta} \qquad (7)$$

Where *Rs* (sample was reflectivity for s-polarized light) and *Rp* (sample reflectivity for p-polarized light) are the reflectance of the s- and p-polarization.

This ratio is a complex number, which is typically denoted by ρ (rho), and is often reported in terms of the Ellipsometry parameters Ψ (Psi), defined magnitude of the reflectivity ratio for p- and s- polarized light, and Δ (Delta), defined the phase difference between the reflected p- and s- polarized. Finally the recording data is transferred to a computer for the calculation of layer thickness and/or refractive indices by optimizing the optical constant and layer thicknesses that generate data curves that best match to the experimental data curves.

Haeberle [27] reported on Al_2O_3 films which were deposited by T-ALD and PE-ALD with controlling substrate temperature during deposition from room temperature to 200°C, and ellipsometry results are shown in Figure 17.

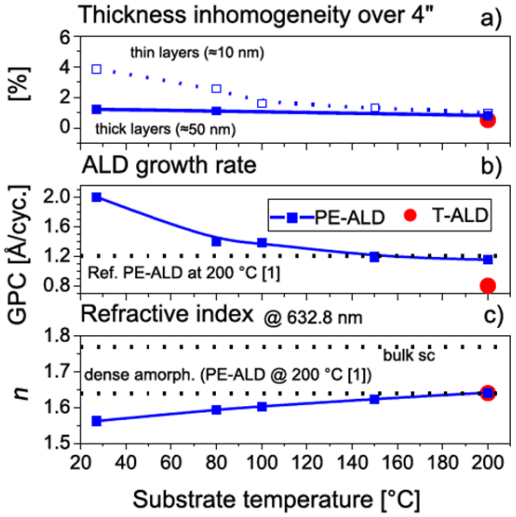

Figure 17 Ellipsometry results showing thickness homogeneity (a) growth rate; (b) refractive index at 632.8 nm; and (c) dependence of the substrate temperature of PE-ALD layers (blue squares, filled: ~50 nm thick films, open: ~10 nm thick films) [27]

5.3 Raman Spectroscopy

Raman spectroscopy is a light scatter technique for analysis of molecules and chemical species based on inelastic scattering of light from laser source. The scattering depends on the fact that some energy from the light is transferred to the vibration modes of the atoms and molecules. Raman spectroscopy can be used for most of non-metallic samples from gases to solids. The technique is non-destructive to most materials [13]. This research prefers using confocal Raman microscopy referring to the ability for sampling in the XY (lateral) and Z (depth) axes. The technique is possible to analyze individual particles or layers which dimension down to 1 μm or below.

Zhang et al. [28] reported on Raman spectra of alumina polymorphs such as nordstrandite,gibbsite, diaspore, boehmite, barite, and α-Al_2O_3. These polymorphs displayed different phonon behaviors, which attributed to their internal crystal structure changing. The strongest Raman peaks of nordstrandite, gibbsite, diaspore, Boehmite, bayerite and α-Al_2O_3 were located at 214.2 cm^{-1}, 3314.4 cm^{-1}, 2298.6 cm^{-1}, 747.7 cm^{-1}, 3484.6 cm^{-1} and 529.2 cm^{-1}, respectively, as shown in Figure 18.

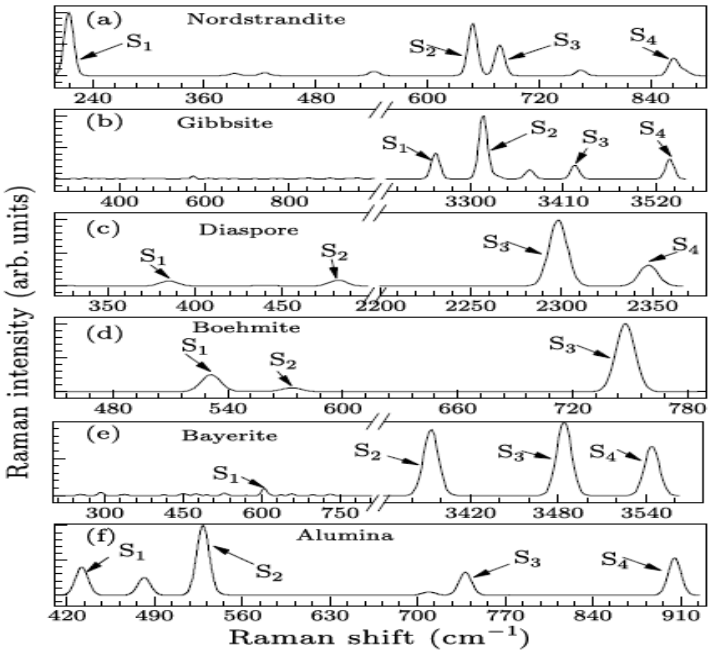

Figure 18 The calculated Raman spectra of polymorphs nordstrandite, gibbsite, diaspore, boehmite, bayerite and α-alumina are displayed in (a)–(f) [28].

5.4 Scanning Electron Microscope (SEM)

Scanning electron microscopy (SEM) is a technique generating high resolution images at various magnifications by focusing electron beam over the surface of the sample and collecting secondary electrons scattered from the sample. Once the beam hits the sample, the electrons interact with the atoms, and sample produce signals that contain information of sample surface topography and composition. The backscattered image gives information with more chemical while secondary electron gives better comprehensible images of the surface. In additional SEM is often equipped with Energy Dispersive Spectrometer (EDS) analysis used for determining the elemental composition of a specimen. This technique measures the energy of characteristic photons emitting from elements in the sample. No sample preparation is required for electrical conductor. The electron beam can damage some samples but in general, it does not destroy the sample [13]. Schematic of SEM is displayed in Figure 19.

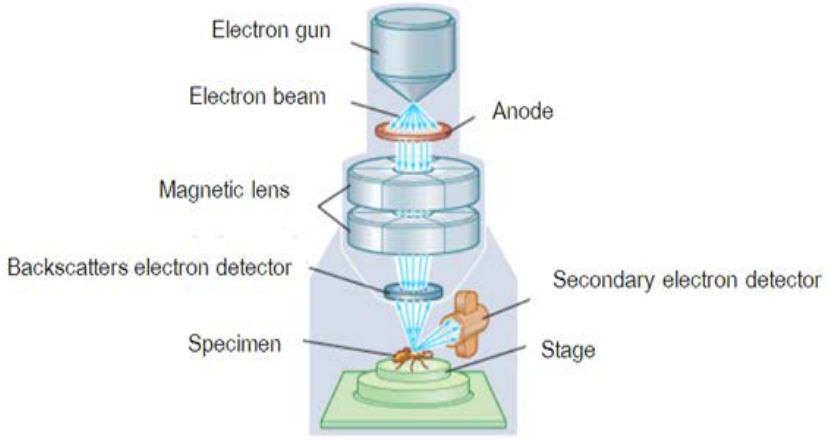

Figure 19 Schematic of Scanning Electron Microscope (SEM).

This research applied SEM for analyzing morphology and elements using SE, EDS mode with acceleration voltage about 0.02 – 30 kV and the characteristic X-rays about 1-3 μm analysis depth. This technique is fast analytics with high resolution.

Wallin et al [29] reported on the synthesis of α-alumina using reactive high power impulse magnetron sputtering (HiPIMS) directly onto cemented carbide and Mo substrates at a temperature as low as 650°C. The microstructure of the coating films was characterized by SEM as shown in Figure 20.

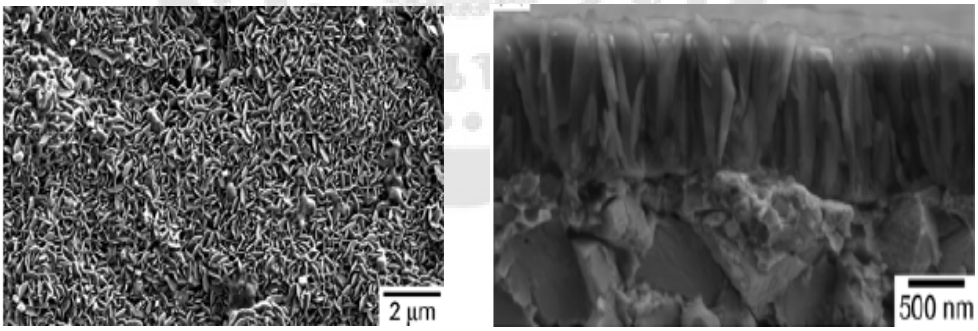

(a) Top view (b) Cross section

Figure 20 SEM images of α-alumina films deposited at 650°C by reactive high power impulse magnetron sputtering at floating substrate bias potential; (a) Top –view; (b) Cross section [29].

5.5 Transmission Electron Microscopy (TEM)

Transmission Electron Microscopy (TEM) is used to observe the microstructure and the composition at the film and substrate interface along the growth direction. The structure and composition information obtain when an electron beam passes through a sample and the transmitted electrons is detected. A high resolution, two-dimensional black and white image creates from the interaction that takes place between prepared samples and energetic electrons in the vacuum chamber. The schematic of TEM is shown in Figure 21. The images can be manipulated by adjusting the voltage of the gun to accelerate or decrease the speed of electrons as well as changing the electromagnetic wavelength via the solenoids. The lighter areas of the image represent the places where a greater number of electrons are able to pass through the sample and the darker areas reflect the dense areas of the object. The preparing sample method can do many ways as dehydration, sputter coating of non-conductive materials, sectioning and staining.

Figure 21 Schematic of Transmission Electron Microscopy (TEM).

In this thesis, interface and thin film compositions examined using TEM (FEI Osiris with super X-EDS Bruker Nano GmbH), including cleaning thin film surface with Nano milling for eliminating contamination or some residue on thin film surface for enhancing the benefit of HAADF scanning for elemental detection.

Katamreddy et al. [30] reported on the synthesis of Al_2O_3 by ALD using Tris (diethylamino) aluminum and water as precursor and applied TEM to define the interface between Si wafer as substrate and Al_2O_3 as target. The films were amorphous layers. TEM image is shown in Figure 22.

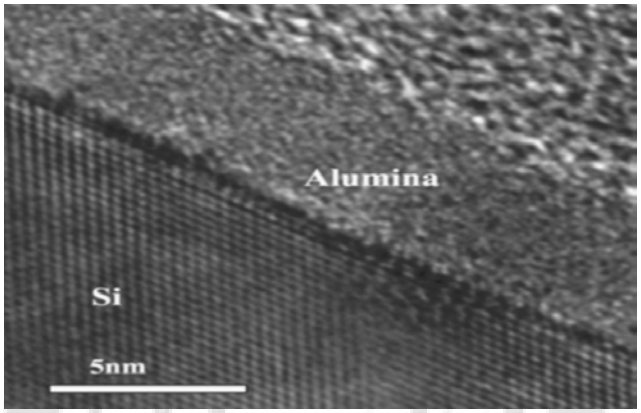

Figure 22 TEM image of as-deposited alumina film, thickness 5.2 nm, on Si wafer using ALD technique [30].

5.6 X-ray diffraction (XRD)

X-Ray Diffraction (XRD) is a technique in which X-ray incident onto the sample surface and the diffracted beams coming out of it is detected. The intensity of the diffracted radiation is dependent on the interaction of the beam with the sample. This technique can identify phase composition; determine the orientation of single crystal or grain, crystal structure of unknown material and measure size, shape, internal stress of small crystalline region of the films [13]. Bragg's law, giving a condition for intensity maxima of the diffracted radiation as a function of the angle θ, is described the principle of the diffraction phenomenon.

$$2d \sin\theta = n\lambda \qquad (8)$$

Where n is an integer, λ is the wavelength of the x-ray radiation, and d is inter planar spacing of the diffracting atomic planes.

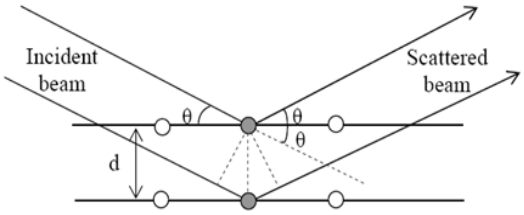

Figure 23 Schematic illustration demonstrating X-ray diffraction according to Bragg's law.

Conventional XRD sometimes is difficult to analyze thin film due to their small diffracting volumes resulting in low diffracted intensities comparing with the substrate and background. This research prefers using the Glancing angle x-ray diffraction (GXRD), that suitable for analysis thin film and the diffraction can be made surface sensitive when need the information lies within a thin layer of the material. Normally this technique can applied for analyzing thin films as thin as 100 Å. For GXRD, the incidence angle is fixed below critical angle of total reflection, typically between 1 and 3° and the angle between the incident beam and the diffracted beam (2 theta) is varied, thus the total external reflected wave penetrates only a few nanometers into the material, giving extremely high surface sensitivity. The GIIXD geometry [31] is shown in Figure 24.

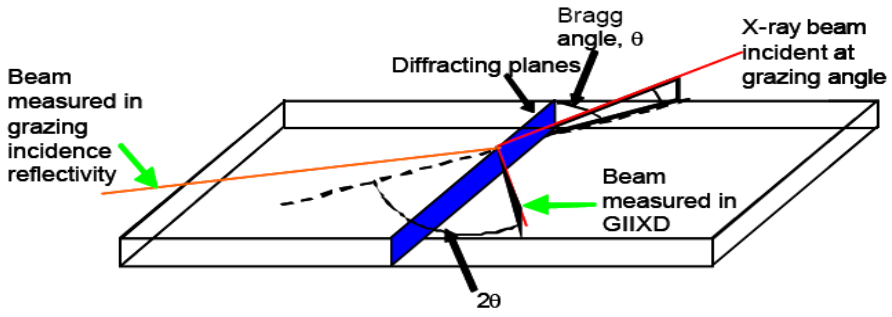

Figure 24 Schematic diagram of the GIIXD geometry, showing the incident and diffracted beam and the reflected beam that was measured in standard grazing incidence reflectivity [31].

Cimalla et al [26] reported on the synthesis of Al_2O_3 thin film which was passed thermal treatments after deposition by PA-ALD. GI-XRD measured after annealing in N_2 at 1050°C. The presence of Bragg reflections clearly indicates the formation of a crystalline AlOx-phase. Best congruence of the measured peak positions found the dominant peak of diffraction intensity at 32°, 46°, and 68° corresponding to δ- Al_2O_3 phase or γ- Al_2O_3 phases of the PDF-2 X-ray powder data. Result is shown in Figure 25.

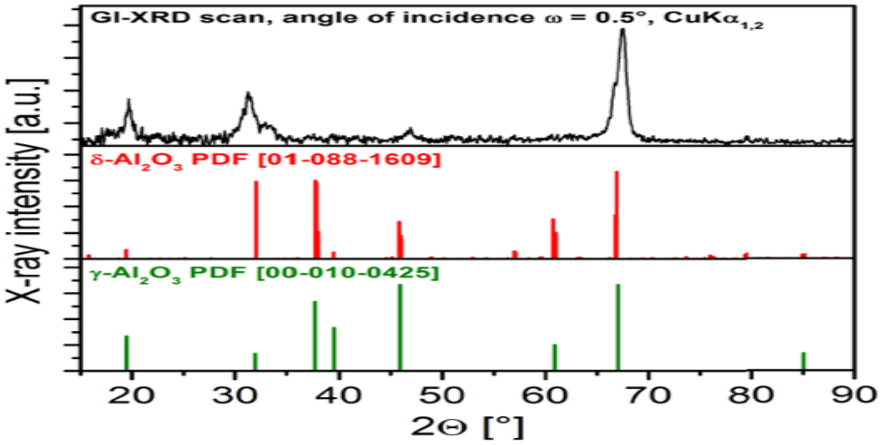

Figure 25 GI-XRD spectra of films after annealing in N_2 at 1050°C [26].

Additionally oxide and hydroxide of aluminum were also reported. Shih and Liu [32] were reported about how thermally-formed oxide, such as gibssite, diaspore, α-Al_2O_3 and possibly γ- Al_2O_3 progressively developed after an extended heating and holding period. Figure 28 presents X-ray diffraction of deposited films when heated in furnace for 2.1 $x10^3$, 6.2$x10^3$, 1.4 $x10^3$, and 2.2 $x10^3$ respectively and subsequently cooled in air. All samples were heated for time responding to A, B, C, and D. The spectra peaks at 2 theta have shown different angle based on oxide and hydroxide of aluminum during transformation. This result also supported Cimalla et al. as presented in Figure 26.

Figure 26 X-ray diffraction powder curves oxide of aluminum [32]

5.7 X-ray Photoelectron Spectroscopy (XPS)

X-ray Photoelectron Spectroscopy (XPS) is a surface spectroscopic technique providing the chemical composition of surfaces by determining what elements exist in a film and determining the electronic, chemical, and physical nature of an element as existing with other elements. XPS data obtains by X-ray irradiation of sample under high vacuum and collecting of electrons ejected from the surface. The deep inner shell electrons are excited, both core, and valence band electrons ejected with characteristic energy and release of x-ray photoelectrons. Electrons emitted from atoms within a few atomic layers of the surface are escapes and energy is analyzed. Results will provide quantitative and qualitative information of the oxidation states of surface and near-surface atoms, surface impurities, and fundamental interactions between surface species [13].

Dechana et al. [23] reported on the measurement of Al atomic percentage using the XPS of Al_2O_3 film deposited by PE-ALD. Based on XPS core level spectra, bulk and interface layer can be fitted by two contributions with binding energy of 74.8 eV and 75.7 eV. The lower binding-energy peak was referring to an octahedral coordination of Al, which was assigning to the bulk Al_2O_3, while higher binding-energy peak corresponded to a

tetrahedral coordination, as shown in Figure 27. The XPS depth profiles could be able to measured atomic percentage of relevant elements of deposition. The ratio of Al:O was approximately 1.7:3 in the bulk Al_2O_3 region. The bulk and the interface regions were relatively comparable. The film thickness for this particular case was about 39 nm, but different thickness also have had similar XPS profiles.

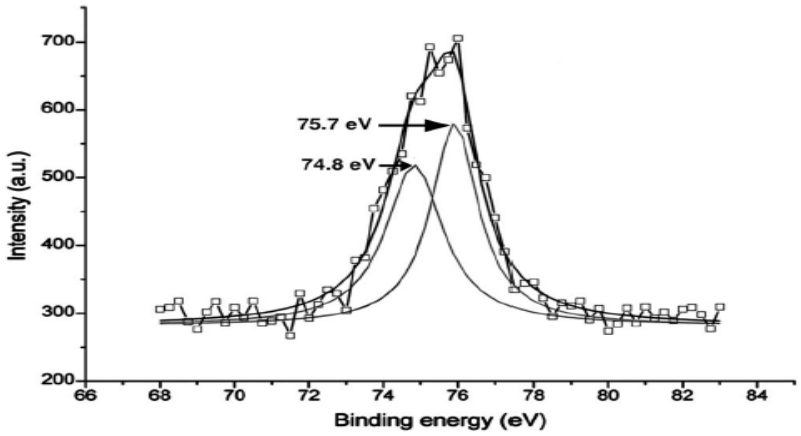

Figure 27 XPS core level spectra of Al_2O_3 film deposited by PE-ALD [23].

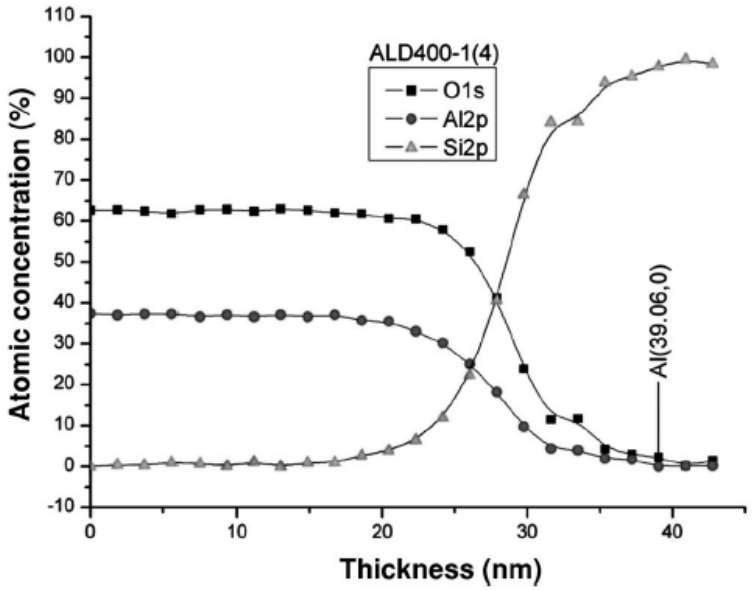

Figure 28 Atomic percentages of elements comprised of Al_2O_3 film deposited by PE-ALD (thickness 39.06 nm) and Si substrate as a function of the film thickness determined by XPS measurement [23].

5.8 Nano indentation

Nano-indentation is a technique used for assessing mechanical properties. It is applicable for measuring the hardness and elastic modulus of a material from indentation load– displacement data obtained during one cycle of loading and unloading as shown in Figure 29**.** The principle of Nano-indentation is pressing a diamond tip with controlling force into the sample surface then records the response of the material. The tip is allowed to penetrate, with increasing force up to a specified maximum load (P_{max}), then the force is slowly decreasing to zero. The penetration to the sample with the reference body firstly leads to elastic deformation, from a certain load an additional plastic deformation occurs. When the specimen is unloading, only the elastic deformation disappears [13].

This research investigated the mechanical properties in term of elastic reduce modulus and hardness. Elastic modulus defined as the ratio stress/strain for tensile stress acting in one direction, while the hardness is a measure of a samples resistance to penetration.

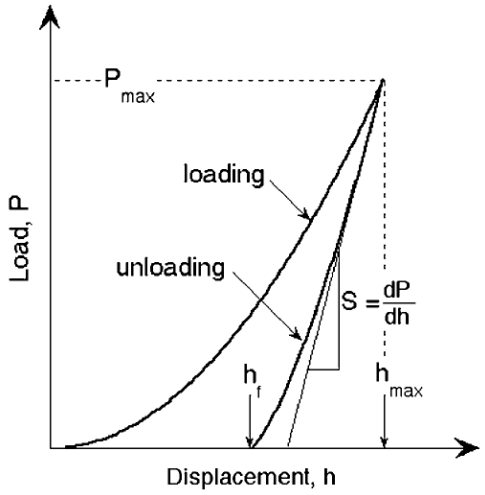

Figure 29 The Principle of Nano indentations technique [33].

Where *S* is the stiffness of the unloading curve and *A* is the projected contact area. The initial unloading contact stiffness (the slope of the initial portion of the unloading curve) is defined by

$$S = \frac{dP}{dh} \tag{9}$$

Where *Pmax* is the maximum indentation force and *A* is the resultant projected contact area at that load. The reduced modulus is defined as:

$$E_r = \frac{S\sqrt{\pi}}{2\sqrt{A}} \tag{10}$$

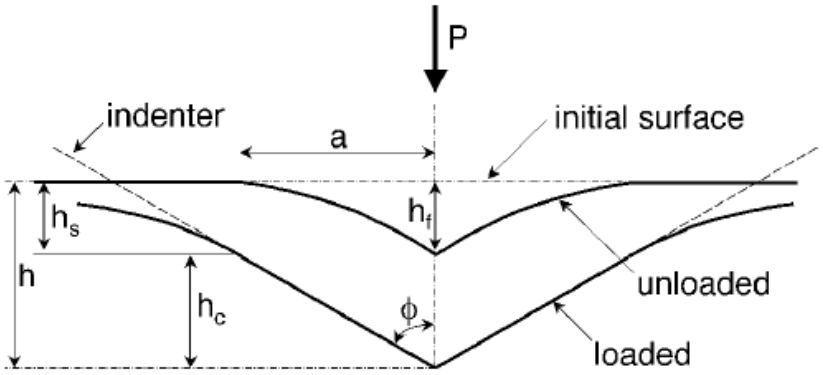

Figure 30 Schematic illustration for the unloading process, showing characteristic parameter of the contact geometry [33].

The contact area is determined from the probe area function A(hc) where hc, the contact depth, is found with

$$h_c = h_{max} - \epsilon\frac{P_{max}}{S} \tag{11}$$

Hardness (H) is defined as the mean contact pressure at the maximum load or total resistance to penetration (elastic and plastic), where A is the project area after loading.

$$H = \frac{Pmax}{A} \qquad (12)$$

Liu et al [34] reported on the improvement of the reliability of Nano indentation hardness measurement of the ALD Al_2O_3 films deposited at controlling substrate temperature at 300°C. The characteristic of the indentation load-displacement responding to the Si wafer substrate under the condition that no plastic deformation occurs is shown in Figure 31.

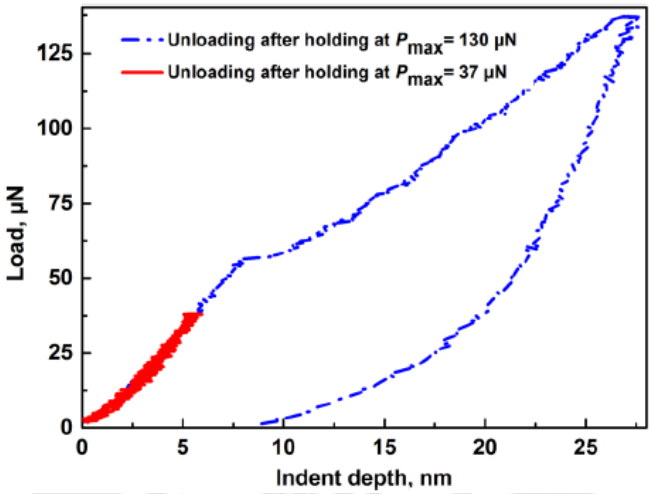

Figure 31 Unloading behavior of the film-free silicon wafer after withdrawal of a tip from the elastic region and from the elastic-plastic region [34].

6. Physical mechanism reviewed

Haeberle et al. [35] reported about alumina film deposited on Si-wafer with T-ALD and PE-ALD using TMA, H_2O as precursor and nitrogen as carrier gas by controlling temperature at 200°C for T-ALD and PE-ALD at room temperature, 80°C and 200 °C. Results have shown SE data (thickness, refractive index, growth rate) correlating to XPS data. T-ALD and PE-ALD film have comparable of refraction index and oxygen to aluminum elemental ratio. However, PE-ALD has increased growth rate when reduced deposition temperature to RT leading to higher carbon content and CH-species.

Katamreddy et al. [30] reported on Al_2O_3 thin film deposited with ALD on Si wafer (100) using Tris(diethylamino) aluminum and H_2O as precursor by controlling substrate temperature at 150–450°C. Al_2O_3 oxide film was amorphous and stoichiometric with no detectable Al–Al cluster formation and no silicate formation at the interface of as-deposited alumina films.

Hahtela et al. [46] reported on the alumina thin film deposited by ALD using TMA, H_2O as precursor and nitrogen as carrier gas by controlling temperature at 220°C. They reported that thin film can deposited on mechanical resonant components without degrading the intrinsic high mechanical quality. The resonant structures leads to the increase in the resonance frequency with increasing film thickness. The reflectivity of silicon was reduced from R Si = 0.35 to RAR = 0.035 at 633 nm by coating the silicon oscillator with an alumina film whose thickness corresponds to the quarter of the optical wavelength serving as a single-layer anti-reflection coating.

Smietana et al. [37] reported on thin aluminum oxide (Al_2O_3) films deposited by ALD using TMA, O_2, as precursor and nitrogen as carrier gas by controlling temperature at 150°C. The deposition onto LPG-based sensing structures induced the optical fibers. Results have shown that the refractive index of the films decreased slightly with the number of the deposition cycles, and the effect could have an influence on the LPG-based device functional properties.

Lee et al. [38] reported on aluminum oxide films deposited by a PE-ALD on Si wafer substrate using TMA, N_2O as precursor and argon as carrier by controlling temperature at 180°C. The study has shown small amount of N accumulated between Si/Al_2O_3 interfaces. After annealing, film became Si_3N_4 bonding and the binding energy was increased. This is likely due to increasing of oxygen content in the interlayer.

Ali et al. [39] reported on morphological and chemical properties of the Al_2O_3 thin films deposited on polymeric substrates by ALD using TMA, H_2O as precursor and argon as carrier gas by controlling temperature at 50°C and 150°C. The surface morphology has been improved with the increasing in deposition temperature and Al_2O_3 film is excellent on insulating properties and shown optical transmittance of more than 85 % in the visible region.

Groner et al. [40] reported on alumina film deposited by ALD using TMA, H_2O as precursor and nitrogen as carrier gas by controlling substrate temperature at 33°C and 177°C. Materials substrates were Si-wafer, PET, quartz crystal microbalance (QCM) sensors. They reported that alumina film can be deposited at low temperature resulting in low surface roughness value, low leakage currents, high dielectric constants, and growth rates in excess of 1Å/cycle. The film was applicable for organic, polymeric, or biological materials.

Shen et al. [41] reported on the growth of Al_2O_3 films by ALD method at room temperature and 300°C using O_3 instead of H_2O employing as oxygen precursor. The Al_2O_3 films surface were atomically smooth. It was found less defects density in the O_3-based Al_2O_3 film than H_2O-based. With excellent insulating behavior, it was suitable for microelectronic devices.

Wang et al. [42] reported on Al_2O_3 thin films deposited by ALD on Si substrate with TMA, H_2O as precursor. They found that the refractive index of Al_2O_3 thin films decreased with increasing film thickness and the changing trend revised after annealing.

CHAPTER III

FILMS PREPARING AND CHARACTERIZATION

This chapter describes the details of methodology using for synthesizing and characterizing of thin Al_2O_3 films formed by Plasma-Enhanced Atomic Layer Deposition (PE-ALD)

1. Materials and equipment for thin film deposition

1. Trimethyl aluminum (TMA, $Al(CH_3)_3$) (SIGMA-ALDRICH)
2. Silicon wafer n- type (1-0-0) (Silicon Quest International)
3. Petri disk polystyrene size 15x 60 mm^2
4. Isopropyl Alcohol (IPA)
5. Distilled water (DI water)
6. Nitrogen gas (N_2) purify 99.9%
7. Oxygen gas (O_2) purify 99.5%
8. Argon gas (Ar) purify 99.9%
9. Beaker size 100 ml
10. Tweezers
11. Nitrile glove
12. Clean wiper

2. Experimental Procedure and Deposition Conditions

Al_2O_3 thin films were deposited on n-type Si wafer substrate by PE-ALD using trimethylaluminum (TMA) and O_2- plasma precursors in the reactor developed by The Plasma and Beam physics Research Facilities (PBP), Chiang Mai University, Thailand. Prior PE-ALD processing, Si wafer were rinsed by IPA to remove residual light organics and subsequently dried with N_2. The Si wafer was then loaded into the ALD reactor. The target holder in the reaction chamber was heated to 80°C, 100°C, and 150°C according to experimental requirement.

2.1 Thin film preparing

Silicon wafer(1-0-0) used as substrate was cut to a size about 1 x 1 cm^2 and then cleaned with IPA and dried with nitrogen (N_2) as shown in Figure 32.

.

Figure 32 Si wafer substrate for deposition processing

2.2 The PE-ALD set up system.

1. The thin films depositions were carried out using PE-ALD system of Chiang Mai University.

2. The plasma source was an inductively coupled plasma source equipped with remote operation.

3. The pressure was kept constant at 3.07×10^2 Pa.

4. Cleaning the reaction chamber prior deposition by purging with argon gas from plasma source for 10 minutes.

5. The microwave power was set to 130 W.

2.3 Thin film synthesis condition

1. Set up the sequence of Al_2O_3 thin films deposition process, one cycle consisted of 1s TMA pulse, 1s Argon purge, 4s O_2 pulse and 1s Argon purge. The flow rates of TMA, and, O_2 were 1.0 and 7.5 sccm, respectively, while the purge Ar flow rate was 1.5 sccm as shown schematically in Figure 33. (Note. sccm is standard cubic centimeters per minute)

2. For the first recipe, the substrate temperature was set to 80°C and the number of coating cycle was varied to 400 or 800 cycles for comparison. The effects of plasma assisted deposition was test, one group of samples were deposited without plasma and the others with plasma. Details of experimental set up are summarized in Table 6.

3. For the second recipe, the number of coating cycle was set to 800 cycles and the substrate temperature was varied between 80°, 100°, and 150° C. The deposition of all cases were done under plasma assisting. Details of experimental set up are summarized in Table 7.

Figure 33 Coating cycle for thin Al_2O_3 film formation using PE-ALD system [23].

Table 6 Details of experimental set up for the first recipe.

Group	Coating cycle	Substrate temperature (°C)	Plasma Condition
1	400 cycles	80° C	without plasma
2	400 cycles	80° C	with plasma
3	800 cycles	80° C	without plasma
4	800 cycles	80° C	with plasma

Table 7 Details of experimental set up for the second recipe.

Group	Coating cycle	Substrate temperature (°C)	Plasma Condition
1	800 cycles	80° C	with plasma
2	800 cycles	100° C	with plasma
3	800 cycles	150° C	with plasma

3 Thin Film characterization

3.1 Surface characterization

1. Atomic Force Microscopy (AFM)

Surface roughness of samples deposited with thin film was measured by Bruker's Dimension Icon® Atomic Force Microscope (AFM) System, using tapping mode. The measurement was set up to scan over the area of 1x1 μm or 10x10 μm depending on each investigation. The scan rate was controlled to 0.999 Hz, tip velocity 2.00 um/s, amplitude set point 18.00 nm, drive frequency 315.815 kHz, drive amplitude 58.90 mV and Z piezoelectric voltage -49.13 V. The virgin sample and the samples deposited with first and second recipes were selected for surface roughness observation. AFM using in this study is displayed in Figure.34.

Figure 34 Bruker's Dimension Icon® Atomic Force Microscope (AFM) System using for measuring the surface roughness of thin films.

2. Spectroscopic Ellipsometry (SE)

The Spectroscopic Ellipsometry is able to use for measuring the thickness of Al_2O_3 films which thickness in the range of sub-nanometer to few nanometers. In this study, the films thickness was estimated by M-2000 Ellipsometer (J.A Woollam Co. Ellipsometry Solution) using SE technique. The value of ψ and Δ were obtained over the spectral range of 240-1000 nm for an incidence angle of 65.2 degree. The obtained value could be able to determine the true Al_2O_3 thickness simultaneously. ALD was growth on a native oxide layer covering Si wafer substrate, thus the oxide layer was measured for comparison. The samples deposited with first and second recipes were selected for films thickness estimation. SE using in this study is displayed in Figure 35.

Figure 35 M-2000 Ellipsometer (J.A Woollam Co. Ellipsometry Solution) using for measuring the film thickness.

3.2 Thin film structure characterization

1. Raman Spectroscopy

Molecular and chemical species of films were analyzed using Jobin Yvon spectrometer, model HORIBA (T64000). Confocal Raman microscopy is possible to analyze individual particles or layers with dimensions down to 1 μm or below. This model equipped with triple monochromator, 532 nm solid state excitation laser, and a focused spot size of about 0.8 μm by a 100X objective (NA = 0.9), was used for the Raman measurements and the spectra were mapped with the library for identification. The virgin sample and the samples deposited with first and second recipes were selected for Raman measurement. The Spectroscopy using in this study is displayed in Figure 36.

Figure 36 JOBIN YVON HORIBA spectrometer, model HORIBA (T64000)

2. Scanning Electron Microscope (SEM)

Surface morphology and elemental composition of thin films were analyzed using a Zeiss Merlin SEM. The samples were attached on carbon stub and loaded into the stage of SEM prior measurement. The virgin sample and the samples deposited with plasma assisting at 100°C and 150°C were observed their morphology using secondary Electron (SE) mode with the magnification of 2 KX. For samples deposited with plasma assisting at 150°C were scanned with higher magnification to 40 KX. EDS equipped with SEM was applied for elemental composition analysis of the samples deposited with plasma assisting at 100°C and 150°C using a constant accelerating voltage at 2 keV. SEM/EDS using in this study is displayed in Figure 37.

Figure 37 Zeiss Merlin SEM/EDS using for surface morphology and elemental analysis.

3. X-Ray Diffraction (XRD)

Phase of crystallinity and film structure were analyzed using Advance x-ray diffractometer (Bruker D8). The spectra were recorded over the range of 10 – 80 degree 2 theta. The virgin sample and the samples deposited with second recipes were selected for XRD measurement. The spectroscopy using in this study is displayed in Figure 38.

Figure 38 Advance x-ray diffractometer (Bruker D8), XRD using for phase and structural analysis.

4. X-ray Photoelectron Spectroscopy (XPS)

Chemical and elemental compositions of thin films were investigated by XPS using AXIS Ultra DLD (Kratos Analytic Ltd.). The XPS spectroscopy was set up with lens hybrid mode with resolution pass energy 80. The samples prepared for this measurement were samples deposited with plasma assisting to 800 cycles at controlling substrate temperature 100°C and 150°C. XPS spectroscopy using in this study is displayed in Figure 39.

Figure 39 AXIS Ultra DLD (Kratos Analytic Ltd.), XPS

5. Transmission electron microscopy (TEM)

The microstructure and elemental compositions of the film/substrate interface along the growth direction were investigated by TEM (Bruker Nano GmbH, Germany). Thin cross-sections of the samples were prepared using the focused ion beam (FIB) milling technique for cutting sample into lamellae shape by ion beam. Transmission electron microscope operated at an acceleration voltage of 200 kV beam of electrons under condition mapping parameter to width 200 pixel, 11nm, Height 300 pixel, 17 nm and pixel size 57 pm including TEM BF Image and HAADF line scan.

NANO milling using for cleaning thin film surface prior perform STEM HAADF scanning by using an energetic 2keV 180pA beams for 8 minutes. The samples selected for microstructural and elemental analysis were deposited with plasma assisting to 800 cycles at controlling temperature 100°C and 150°C. Both samples were coated with CrO_2 prior milling process via FIB. TEM using in this study is displayed in Figure 40.

Figure 40 TEM (Bruker Nano GmbH, Germany) using for microstructural and elemental analysis.

3.3 Mechanical Properties

Nanoindentaion (Hysitron) using Berkovich tip was applied for investigate three the mechanical properties of deposited film, i.e. hardness (H), Elastic reduced Modulus (Er), and contact depth (hc). Virgin Si wafer substrate and commercial Al_2O_3 films were measured for comparing. The samples deposited with the first recipe were measured with 70 μN force. While the samples deposited with the second recipe were measured with 100 μN force. Nano-indentation using in this study is displayed in Figure 41.

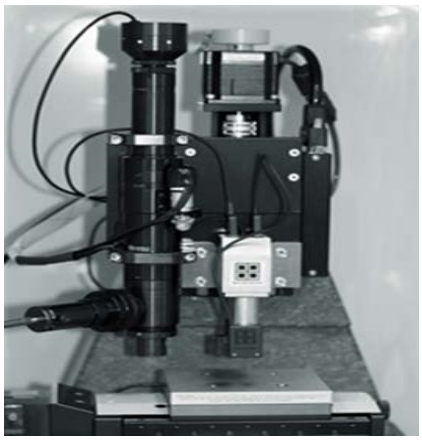

Figure 41 Nanoindentaion (Hysitron) using for investigation the mechanical properties of thin film.

CHAPTER IV

RESULTS AND DISSCUSSIONS

Results of the thin film synthesis

4.1 Surface characteristic

To determine the sample surface information the Atomic Force Microscopy (AFM) using tapping mode was applied for obtaining the surface roughness and the film thickness. The main advantage of this mode is the reduction of forces, leading to less damage to the sample surface and higher lateral resolution. The deposition conditions were controlled for with or without plasma during deposition and controlling coating cycles to 400 or 800 cycles at heating temperature 80°C. Additionally, Ellipsometry provides a very robust procedure to obtain the film thickness measurements which are accurate up to an atomic layer. The spectroscopy was scanned over the wavelength of 240 to 1000 nm and the incident angle of the light was set to 65.2 degrees.

The surface roughness of thin film deposited on Si wafers is usually increased with the deposition temperature. In this study, the roughness appeared to be relatively similar to the Si wafer substrate indicating a very smooth coating with good roughness reduction. The root mean square roughness (Rq) of all samples was ~0.2 nm. It seems that the coating cycle did not affected to the surface roughness of both deposition with or without plasma and also no difference in surface morphology between the initial SiO_2 layer of Si wafer substrate and films deposited without plasma.

For the thickness of films deposited at 80°C with controlling coating to 400 and 800 cycles, the results shown trend of increasing with coating cycles. Moreover deposition with plasma obtained the film thickness thicker than deposition without plasma. Not surprisingly, due to the fact that the plasma enhances the surface energy facilitating the film formation. The measurements of the surface roughness and the film thickness were summarized in table 8

Table 8 Summarization of surface characteristic of Al_2O_3 thin film deposited on Si substrate at 80°C using PE-ALD technique as compare with Si substrate.

Deposition conditions	Surface roughness (nm)			Film thickness (nm)
	Ra	Rq	Rmax	
Si wafer (virgin)	0.191	0.240	2.320	1.87
400 cycles without plasma	0.171	0.214	2.200	2.00
400 cycles with plasma	0.178	0.258	4.660	2.21
800 cycles without plasma	0.186	0.263	4.620	2.41
800 cycles with plasma	0.184	0.290	5.500	2.59

3D AFM images are able to unveil the surface morphology of deposited samples comparing with Si wafer substrate. In this experiment, AFM images revealed the islands formations on samples deposited with plasma to both 400 and 800 cycles as seen in Figure 42 (c), (e). The thickness of Si-wafer substrates was estimated to be ~1.87 nm. This should be belonging to the remaining native oxide layer after standard sample cleaning. After deposition to 400 cycles, the thicknesses were ~2.21 and ~2.00 nm for with and without plasma respectively, while increasing coating cycle to 800 cycles, the thickness were ~2.59 and ~2.41 nm for with and without plasma respectively.

(a) Virgin Si wafer

(b) 400 cycles without plasma

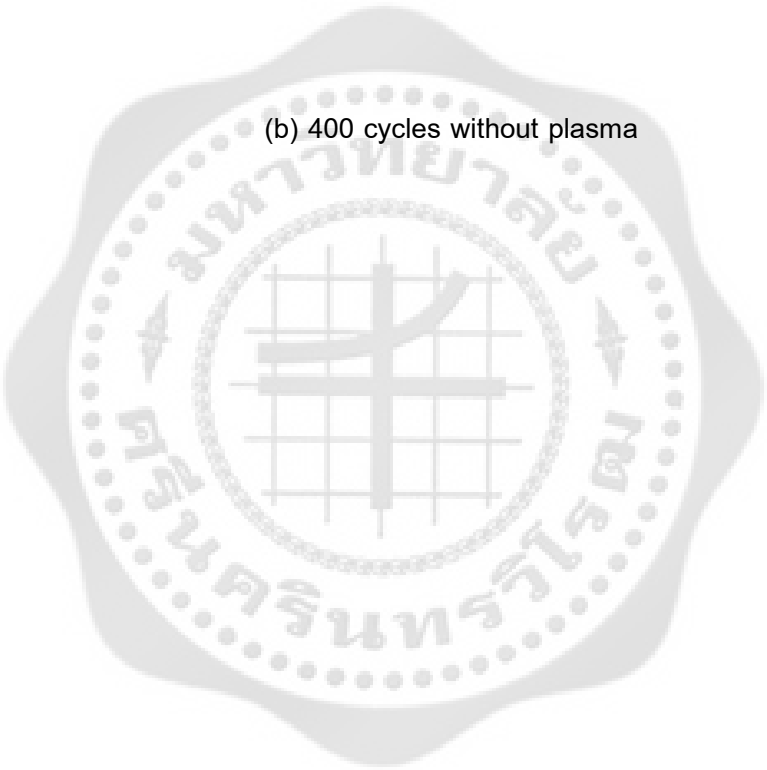

(c) 400 cycle with plasma

(d) 800 cycle without plasma

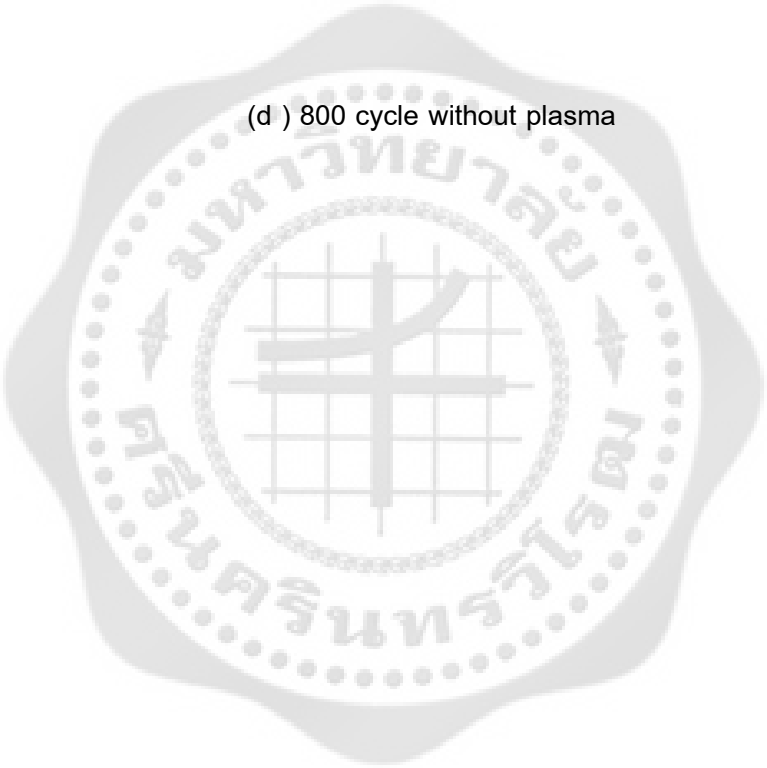

(e) 800 cycle with plasma

Figure 42 AFM 3D images of; (a) Si wafer substrate; and samples deposited at 80°C with (b) 400 cycle without plasma, (c) 400 cycle with plasma, (d) 800 cycle without plasma, (e) 800 cycles with plasma.

Further study was focused on the investigation of the surface roughness and the thickness of films deposited by controlling coating cycles to 800 cycles with plasma condition. In this series, substrates temperatures during deposition were controlled to 80°C,

100°C, and 150°C. Effects of substrate temperature with respect to the film thickness and the (Rq) roughness are reported in Table 9. The films thicknesses were estimated to be 3.53 nm, 5.95 nm and 4.59 nm for deposition at 80°C, 100°C, and 150°C, respectively.

The thickness measurement was able to determine the growth per cycle (GPC) of the ALD process with increasing substrate temperature from 80°C to 100°C and 150°C. According to result the sample deposited at 150°C has lower film thickness than another conditions, it was suspect that the reaction between TMA and substrate surface was not efficiency at this temperature. The aluminum atoms, directly relating to the density of hydroxyl groups on substrate surface, act as adsorbent the molecules of TMA. However, the surface density of hydroxyl groups might decrease with increasing deposition temperature. The surface roughness as reflect from the root mean square (Rq) value was measured by scanning over the area of 10 μm x 10 μm. The Rq of samples deposited at 80°C, 100°C and 150°C were 0.44, 0.36, and 0.51 nm respectively. The increasing of the Rq roughness was attributed to the formation of the crystalline structure which was found like islands of some particle clustering on the substrate surface. 3D AFM images presenting the islands formation of samples deposited at 80ºC, 100ºC, 150ºC are shown in Figure 43.

Table 9 Summarization of surface characteristic of samples deposited with Al_2O_3 thin film for coating to 800 cycles with plasma and substrate temperatures during deposition controlled at 80°C, 100°C, and 150°C.

Deposition conditions	Surface roughness (nm)			Film thickness (nm)
	Ra	Rq	Rmax	
80°C	0.21	0.44	9.18	3.53
100°C	0.23	0.36	8.97	5.95
150°C	0.29	0.51	11.80	4.59

(a) 800 cycles at 80°C

(b) 800 cycles at 100°C

(c) 800 cycles at 150°C

Figure 43 Comparison of AFM 3D images of samples deposited to 800 cycles with plasma by varying substrate temperarure during deposition to; (a) 80°C; (b) 100°C; and (c) 150°C.

The sample surface morphology was examined by Scanning Electron Microscopes with a Zeiss Merlin SEM using Secondary Electron (SE) mode. The experiment focused on comparing the samples deposited at 100°C and 150°C with Si wafer substrate. The magnification was set to 2 KX for all samples and higher magnification (40 KX) only for 150°C sample. The images are shown in Figure 44. SEM image, when increasing the magnification to 40 KX, has shown some particles clustering for sample deposited at 150°C as seen in Figure 44 (d).

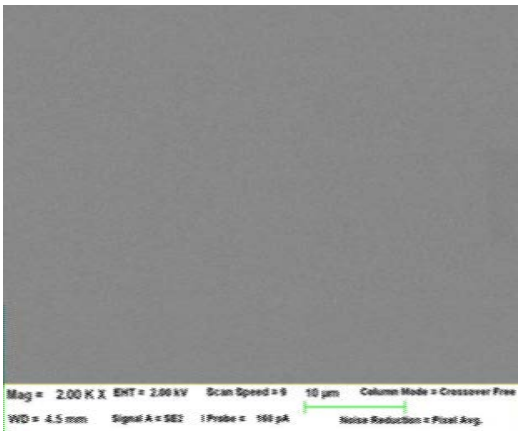

(a) Si substrate (virgin : no coating) (2 KX magnification)

(b) Sample deposited at 100°C (2 KX magnification)

(c) Sample deposited at 150°C (2 KX magnification)

(d) Sample deposited at 150°C (40 KX magnification)

Figure 44 SEM images of samples; (a) si substrate (virgin – no coating), (b) deposited at 100°C, (c) deposited at 150°C (2 KX), and (d) deposited at 150°C (40 KX).

4.2 Thin film structure characteristic

Molecular species

Molecular species of thin films were investigated by Raman spectroscopy using Jobin Yvon spectrometer HORIBA (T64000), equipped with triple monochromator, 532 nm solid state excitation laser, and a focused spot size of about 0.8 μm by a 100X objective (NA = 0.9). Figure 45 exhibits Raman spectra of Si wafer substrate and the sample deposited without plasma to 800 cycles at 80°C and samples deposited with plasma to 800 cycles at 100°C and 150°C. For the virgin Si-wafer, the spectrum displays peaks of the first

(TA) and second (2TA) order transverse acoustical phonon modes from the crystalline silicon structure at ~520 and ~302 cm^{-1}, respectively.

(a) Raman spectra in the 200–400 cm^{-1} region

Figure 45 (a), for Raman spectra in the 200–400 cm^{-1} region, a clear peak due to the second order transverse acoustical phonon (2TA) appearing at ~302 cm^{-1} is presented in the virgin sample. As for Raman spectra of the samples deposited with thin film, the bands in the 200–400 cm^{-1} region are modified and the peak shifted from ~302 cm^{-1}, indicating that the substrate surface was being highly damaged.

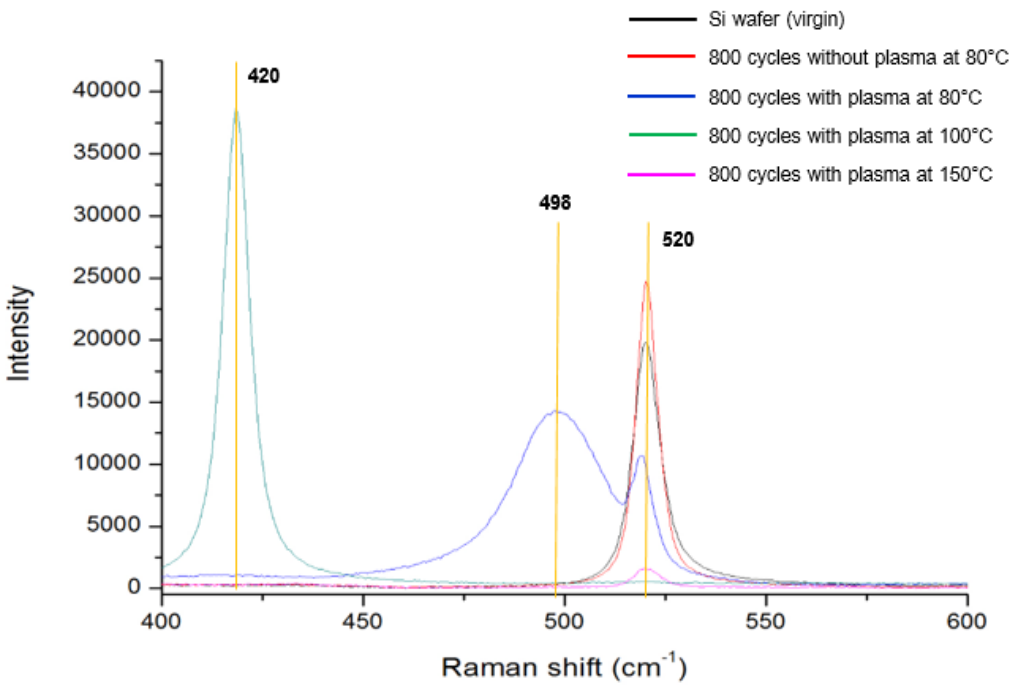

(b) Raman spectra in the 400–600 cm^{-1} region

Figure 45 (b), for Raman spectra in the 400–600 cm^{-1} region, samples deposited with thin film at 80°C with plasma exhibit two sharp peaks centered at ~498 and ~520 cm^{-1}, while samples deposited with thin film at 100°C with plasma exhibit a sharp peak centered at ~420 cm^{-1}. As for sample deposited with thin film at 150ºC, Raman spectra exhibit a sharp peak centered at ~520 cm^{-1} and the peak has lower intensity than other conditions. The Raman spectra of sample deposited with thin film at 80°C without plasma exhibit the sharp peak centered at ~520 cm^{-1} as similar as that of the Si wafer substrate. It might be because film delamination during measurement.

(c) Raman spectra in the 600-1000 cm^{-1} region.

Figure 45 (c), for Raman spectra in the 600-1000 cm^{-1} region, the Si second-order feature appearing at ~970 cm^{-1} of all samples deposited with thin film are greatly modified. The peak shifted away from ~970 cm^{-1}, implying the appearance of other structures.

Figure 45 Raman spectra of samples deposited with thin film to 800 cycles with and without plasma by controlling the substrate temperature at 80 ºC and samples deposited with thin film at 100 ºC and 150ºC with plasma in the range of; (a) 200–400 cm^{-1} region; (b) 400–600 cm^{-1} region; and (c) 600-1000 cm^{-1} region.

Note that the first TA band of Si crystalline structure was detected at ~520 cm^{-1} even after film deposition. This means that the film should be very thin allowing the excitation laser penetrated deep into the substrate material.

The Raman spectra features of samples deposited by PE-ALD indicated that the films consisted of Al-O-Si structure. Based on the literature reviews, it points out that these features might be chemical structure of diaspore mixed with alumina. Diaspore is one structure of aluminum oxide hydroxides which can growth at temperature lower than 400°C [14]. The Raman spectra of diaspore have peaks located at 498 and 2298 cm^{-1} [28]. These peaks match very well with spectra of samples deposited by PE-ALD at 80°C which display a sharp peak centered at ~498 cm^{-1}.

Crystal structure

XRD measurements were performed with the Bruker D8 Focus X-ray diffractometer. The spectra were scanned in 2-theta range of 10 – 80 degree. The XRD patterns of investigated samples are demonstrated in Figure. 46. The dominant features of samples deposited to 800 cycles with plasma and controlling temperature at 80°C, 100°C and 150°C were reproduced extremely well, including the shapes, positions, and widths of the ~69° 2θ band and the ~12° 2θ peak and also contained a slight bump centered ~28° 2θ. Note that the XRD peaks of sample deposited at 150°C was not cleared. It might be the unsmooth surface effecting to the XRD measurement.

The present of these features clearly indicates the existing of a crystalline AlO_x-phase. Because of the broadened and weak peaks reflecting in the Raman spectra implying of the thin layer thickness and possibly incomplete crystallization, thus the unambiguous identification of the exact AlO_x phase is not possible. Moreover, there are a large number of different phases in the material system of Al-O family. In this study, the spectra match with the α-Al_2O_3, δ-Al_2O_3 and γ-Al_2O_3. According to literature reviews, α-Al_2O_3 structure in most cases XRD spectra exhibited peaks at 25, 32, 37, 43, 61 and 68° 2 theta while γ-Al_2O_3 shown the dominant peaks of diffraction at 46, 67, and 85° 2 theta [26,32]. Comparing with the work of Teng-Shih Shih and Zin-Bou Liu [32], reporting about how thermally formed oxide film progressively developed on the surface and after an extended annealing, the XRD peaks appeared at difference angle. It might be because the oxide and hydroxide of aluminum films were transformed during heating.

In concluding the appearance of the peak at 68° 2 theta indicates that the films can be diaspore, α-Al_2O_3, or γ-Al_2O_3. Note that diaspore can transformed to corundum (α-Al_2O_3) at temperature higher than 450°C with the pressure varied from 15000 to 30000 psi [32].

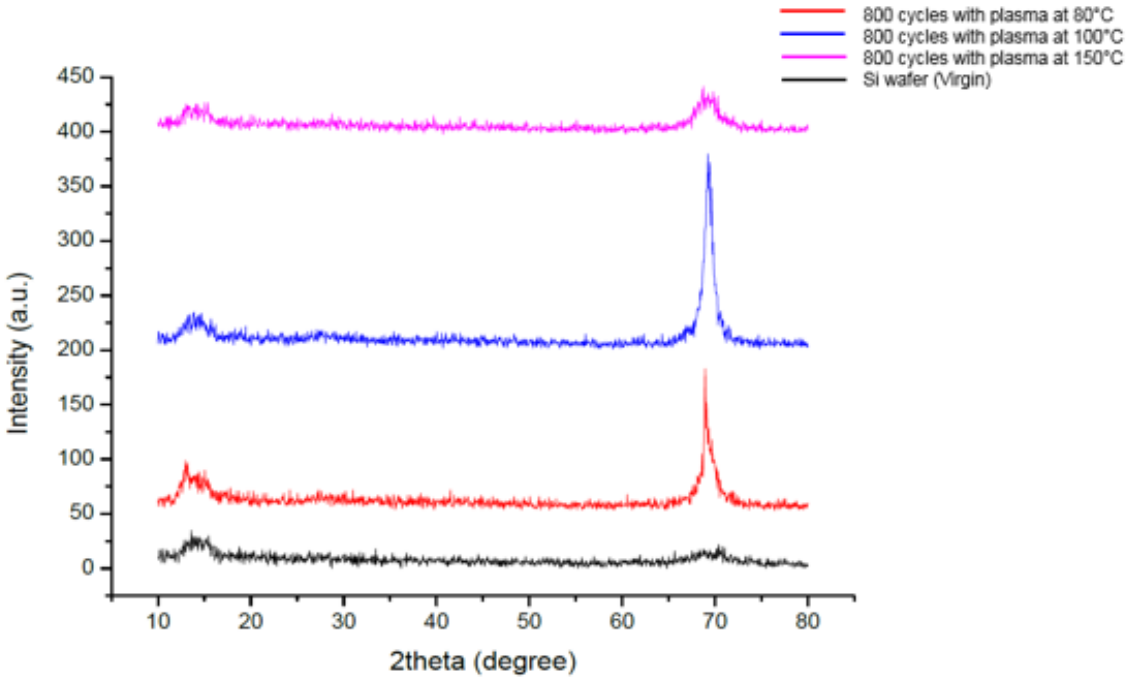

Figure 46 XRD patterns of Si wafer substrate and samples deposited to 800 cycles by controlling the substrate temperature during deposition at 80°C, 100°C, and 150°C.

Chemical composition

Chemical compositions of thin films were investigated by XPS using AXIS Ultra DLD (Kratos Analytic Ltd.). XPS was set up to lens hybrid mode with resolutions pass energy 80. The XPS results revealed that the samples deposited with thin film at 80°C, 150°C contained high percentage of atomic carbon, while deposited at 100°C contained high percentage of atomic silicon as summarized in Table 10. Deposition temperature has effected to the carbon content of the films. The present of carbon in the films is due to organometallic nature of the TMA precursor. Note that aluminum was not detected in all deposition conditions. It might be some contaminations formed during deposition and remained strongly on the sample surface, thus exciting X-rays could not be able to penetrate through these structures. It should combine ion milling with XPS for next experiment to get rid of these structures, thus exposing the real film to X-rays. Surface, thus exciting X-rays could not be able to penetrate through these structures. It should combine ion milling that may effected with the performance of XPS for next experiment to get rid of

these structures, thus detection that can't penetrated to thin film surface exposing the real film to X-rays

Table 10 Summarization of chemical compositions of samples deposited to 800 cycles by controlling temperature at 80°C, 100°C, and 150°C as measured by XPS.

Conc%	Peak	Na 1s	Zn 2p	O 1s	N 1s	C 1s	Si 2p
	Position BE (eV)	1071	1021	532	399	284	99
Atomic	80ºC	0.78	ND	30.63	3.76	43.67	21.15
	100ºC	ND	0.00	37.36	ND	11.86	50.79
	150ºC	ND	0.00	30.64	2.01	43.92	23.43
Mass	80ºC	1.07	ND	29.19	3.14	31.23	35.37
	100ºC	ND	0.00	27.59	ND	6.57	65.84
	150ºC	ND	0.00	28.77	1.65	30.96	38.61

Note: ND= not detectable.

XPS survey spectrum in Figure 47 reveals the O 1s, C 1s, and Si 2p of samples deposited with thin film by PE-ALD using TMA as precursor of alumina.

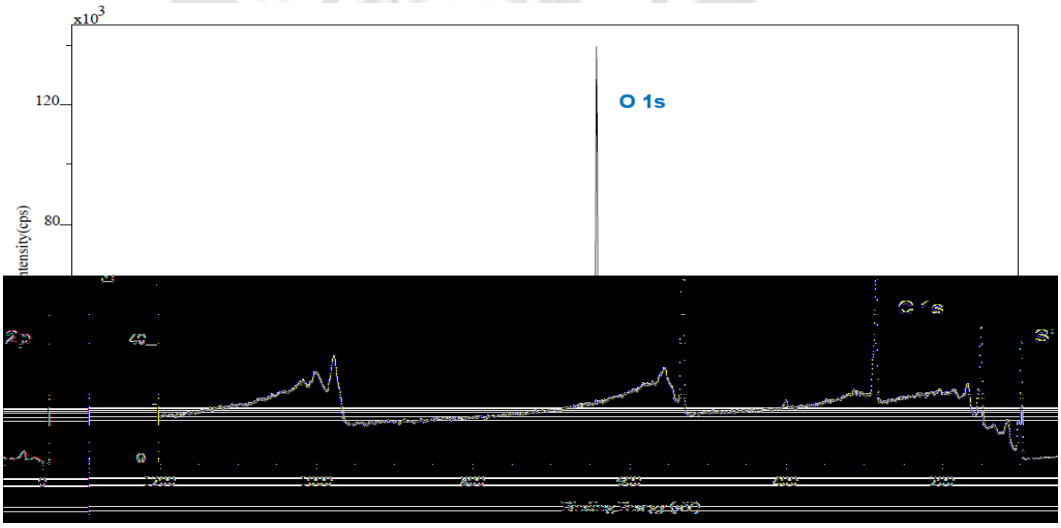

Figure 47 XPS survey spectrum of samples deposited with thin film on Si substrate by PE-ALD technique.

Interface and thin film composition

The morphologic and compositional of thin films were investigated by TEM using FEI Osiris with super X-EDS Bruker Nano GmbH, Germany. Prior measurement, the samples were coated with CrO_2 and cut to lamellae shape by using the Focus Ion beam samples preparation (FIB) milling. Images were done using an energetic 200 keV electron beams under mapping parameter width 200 pixel, 11nm, Height 300 pixel, 17 nm and pixel size 57 pm with TEM BF Image and HAADF line scan modes. Some samples were prepared with the Nano milling for cleaning the sample surface before performing STEM HAADF scanning by using an energetic 2keV 180pA beams for 8 minutes.

Figure 48 TEM image using HAADF scanning mode.

As seen in Figure 48, TEM image clearly displays the interface between Al_2O_3 thin film, SiO_2 layer and Si substrate. The SiO_2 and Al_2O_3 layers were appeared in difference contrast in the micrograph and it can be used to estimate the thickness of the film layer by using HAADF profile maker. The thickness of Al_2O_3 thin film deposited to 800 cycles with plasma by controlling temperature at 150°C was about 1.11 nm. TEM BF images of samples deposited with thin film at 80°C, 100°C, and 150°C were displayed in Figure 49. As seen in Figure 49 (a),

TEM BF image of sample deposited with thin film at 80°C, the Al_2O_3 film was hardly seen. However, Al_2O_3 films were clearly seen in the samples deposited at 100°C and

150°C as seen in Figure 49 (b) and (c) respectively. For the latter cases the interface between Al_2O_3 and Si substrate can be defined.

(a) Deposition at 80°C

(b) Deposited at 100°C

(c) Deposited at 150°C

Figure 49 TEM images of samples deposited with thin films at; (a) 80°C; (b) 100°C, and (c) 150°C.

The EDX equipped with scanning transmission electron microscopy (STEM) was performed for investigation of chemical composition. The solid lines in the Figure 50 (a), (b) and (c) correspond to EDX line scans for samples deposited with thin film at 80°C, 100°C, and 150°C respectively. The signals of all the observed chemical species (Cr, O, C, Si, Ca, Cu and Al) of EDX line scans have shown the same trend to the total signal from the HAADF detector.

(a) Deposition at 80°C

(b) Deposited thin film at 100°C

(c) Deposited thin film at 150°C

Figure 50 XEDS line mapping of samples deposited with thin film to 800 cycles with plasma at heating temperature; (a) 80ºC; (b) 100ºC (c); and (c) 150ºC.

Nano-milling technique is a cleaning surface method that can eliminate contamination covering the films. This technique was applied prior performing STEM HAADF scanning by using an energetic 2keV, 180pA beams for 8 minutes. Samples surfaces after Nano-milling were smooth and films clearly defined as shown in Figure 51.

Elements comprised in thin films were characterized by XEDS mapping scan. Two areas were selected for investigation, mapping 1 as shown in Figure 51 (a) for smooth surface and mapping 2 for rough surface as shown in Figure 51 (b). Note that some clusters were found on top of the surface of the latter case.

(a) Deposition at 150°C after nano milling (Mapping1)

(b) Deposition at 150°C after nano milling (Mapping 2)

Figure 51 TEM image of XEDS for samples deposited with thin films at 150°C after nano-milling of; (a) Mapping 1 smooth surface; (b) Mapping 2 cluster/rougth surface.

For both areas, XEDS mapping are displayed in Figure 52. The mapping 2 for cluster/rough surface area exhibits stronger Al peak than mapping 1 for smooth surface.

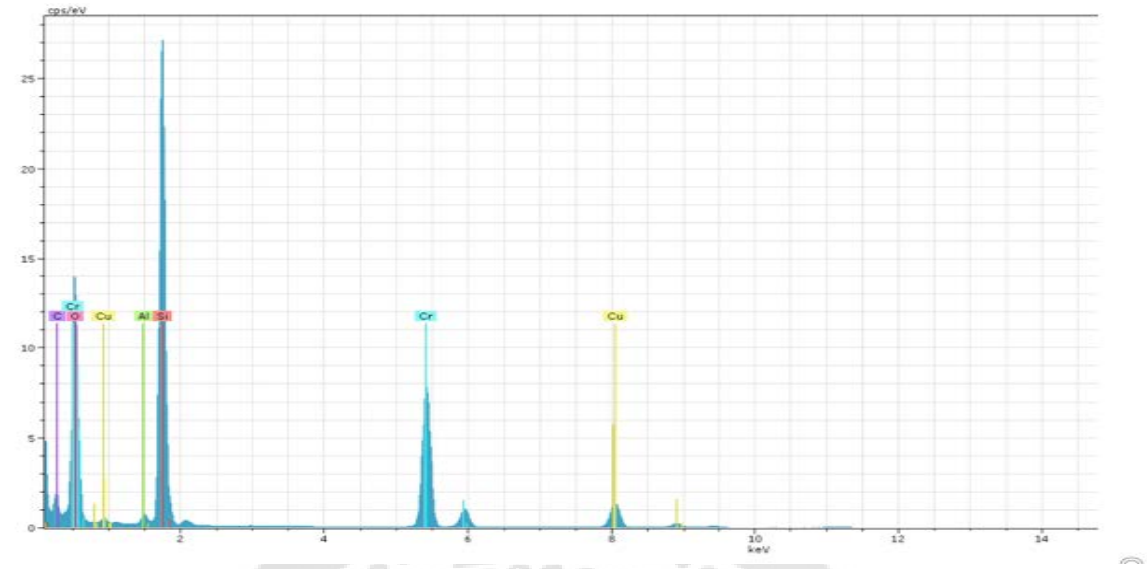

(a) Mapping1 (smooth surface)

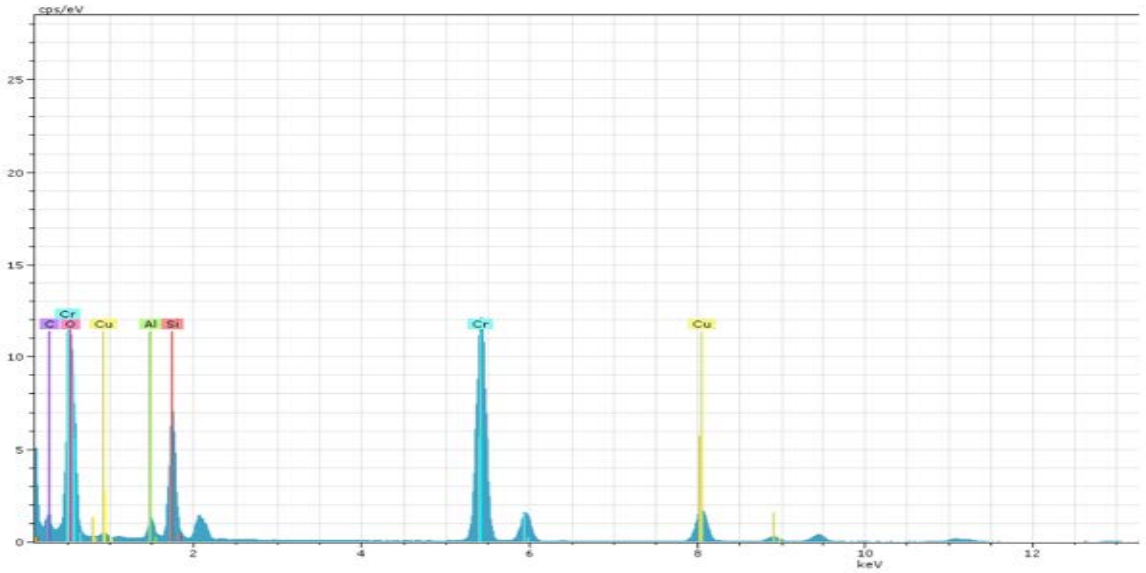

(b) Mapping 2 (cluster/rough surface)

Figure 52 XEDS line mapping of samples deposited with thin film to 800 cycles with plasma at substrate temperature 150ºC for; (a) mapping 1 smooth surface; (b) mapping 2 cluster/rough surface.

Elemental compositions of samples deposited with thin films to 800 cycles at controlling teperature at 80ºC, 100ºC, and 150ºC via XEDS mapping are summarized in Table 11. Al wt% of these samples was estimated to be 0.33%, 0.43%, and 0.51% respectively indicating of temperature effects. Increasing of temperature during film growth

affects to the film microstructure, for example increasing mobility of the species in the reaction. It was reported that only the subsequence thermal annealing could be able to convert the amorphous structure to crystalline form.

Table 11 wt% elements of samples deposited with thin film measured via XEDS mapping by TEM.

Temperature	Wt.%						
(º C)	Aluminum	Argon	Carbon	Oxygen	Silicon	Chromium	Copper
At 80ºC	0.33	0.33	62.45	12.55	14.35	4.87	5.11
At 100ºC	0.43	0.11	47.86	20.96	19.97	9.87	3.80
At 150ºC	0.51	0.12	37.89	20.41	29.11	7.66	4.30

The elemental compositions of samples deposited to 800 cycles with plasma at 150°C after performing Nano milling process are summarized in Table 12. Wt% of aluminum based on XEDS mapping by focusing on the smooth surface area (mapping 1) and cluster/rough surface (mapping 2) contain 0.66% and 1.54% respectively. Nano milling process improves the cleanliness of the films by eliminating some contaminations that remained on films. These features is obstruct to the elemental detection of actual films. Thus, this process should be performed prior STEM scanning for increasing the efficiency of detection.

Table 12 wt% of elements of samples deposited with thin film after Nano milling via XEDS mapping by TEM

MAPPING	Wt.%						
LOCATION	Aluminum	Argon	Carbon	Oxygen	Silicon	Chromium	Copper
Mapping 1	0.66	0.00	30.09	16.38	30.68	16.64	4.64
Mapping 2	1.54	0.00	31.31	14.39	10.54	34.22	8.00

Elements of deposited thin films

The elements comprised of deposited films were measured using a Zeiss Merlin SEM with EDS mode. Figure 53 displays EDS spectra of Si virgin substrate and samples deposited with thin films. For Si virgin substrate, the spectrum displays only Si peak as expect as seen in Figure 53 (a). The EDS spectra of samples deposited with thin films at 80°C display peaks of Si and C as seen in Figure 53 (b) and samples deposited with thin films at 100°C display peaks of C, O, and Si as seen in Figure 53 (c), while samples deposited with thin films at 150°C display Al, Si, C, O and Na and Mg elements as seen in Figure 53 (d).

(a) Si substrate

(b) Deposition at 80°C

(c) Deposition at 100° C

(d) Deposition film at 150°

Figure 53 SEM/EDS spectra of; (a) Si substrate; and samples deposited with thin film at (c) 80°C, (c) 100°C, and (d) 150°C.

4.3 Mechanical Properties

Nano-indentation (Hysitron) using Berkovich tip was applied for mechanical properties testing in term of the relative hardness and elastic reduced modulus. The hardness is the resistance of a material and is directly related to the elastic modulus of the materials, which in turn is dependent on the nature of the chemical bonding and crystal structure of the material. Moreover contact depth is determining the distance of probe that penetrated into

thin films corresponding to the hardness properties. Samples deposited with thin films at 80 °C to 400 and 800 cycles for with and without plasma during deposition were selected for test under force 70 μN.

Table 13 is summarized the hardness (H), Elastic reduced Modulus (Er), and contact depth (hc) of all samples. The Si-wafer substrate was also measured for comparison. The hardness of sample deposited without plasma did not change much as compare with the virgin sample. It is not surprise since the Al-O material system could not be able to form without oxygen atmosphere. As for deposition with plasma, the samples deposited to 800 cycles have higher hardness than that of 400 cycles. Graphical of contact depth with loading using 70 μN indentation forces of these measurements are shown in Figure 54.

Table 13 Summarization of mechanical properties of virgin and samples deposited with and without plasma and controlling substrate temperature at 80°C under force 70 μN.

Deposition conditions	H (GPa)		Er (GPa)		Hc (nm)	
	Mean	Std Dev	Mean	Std Dev	Mean	Std Dev
Si wafer (virgin)	7.13	0.46	113.84	6.03	7.06	0.29
400 cycles without plasma	7.23	0.40	105.92	3.50	7.00	0.31
400 cycles with plasma	6.55	0.64	104.88	6.55	7.60	0.63
800 cycles without plasma	7.13	0.40	107.62	4.22	7.09	0.30
800 cycles with plasma	7.35	0.49	109.13	4.33	6.94	0.39

Note: H = Hardness, Er = Elastic Reduced Modulus, hc = Contact depth.

Further investigation of hardness, elastic reduced modulus, and contact depth was focused on comparison of samples deposited with plasma to 800 cycles and controlling temperature at 80°C,100°C and 150°C. The tests were done under 100μN force using Berkovich tip. The results are displayed in Table 14. Hardness, elastic reduced modulus, and contact depth have the same trend, i.e. increase with increasing temperature of deposition.

Table 14 Summarization of mechanical properties of samples deposited to 800 cycles and substrate temperature during deposition at 80°C, 100°C, 150°C under force 100 μN.

Deposition conditions	H (GPa)		Er (GPa)		Hc (nm)	
	Mean	Std Dev	Mean	Std Dev	Mean	Std Dev
Si wafer (virgin)	7.35	1.43	125.5	19.81	9.75	1.93
80°C	7.86	0.38	117.79	3.18	8.88	0.41
100°C	10.96	3.38	174.38	55.90	7.18	2.00
150°C	10.60	1.21	187.42	34.76	6.96	0.64

Note : H = Hardness, Er = Elastic Reduced Modulus, hc = contact depth

Figure 54 Contact depths of investigated samples using 70 μN indentation forces.

Figure 55 Contact depths of investigated samples using 100 μN indentation forces.

Figure 55 displays graphical of contact depth with loading using 100 μN indentation forces of investigated samples. The contact depth of 150ºC deposition to about 6.96 nm was the lowest if compare with Si substrate and other deposition conditions. It might be because the film delamination during measurement. However, deposition process clearly improves the mechanical properties of Si wafer, e.g. increasing of hardness and elastic modulus.

Figure 56 comparing the mechanical properties (hardness, elastic modulus and contact depth) of all samples in term of the film thickness. It seems that the elastic properties of ALD aluminum oxide depend on its thickness. Films can withstand large strains without cracking to some extend if the thickness reduces. Compare the surface roughness and the film thickness of Si wafer substrate and samples deposited with thin film at 80°C, 100°C, and 150°C leading to conclusive explanation. For overall comparison, surface roughness (Ra, Rq), thickness, elastic modulus, and hardness were increased upon an increasing of substrate temperature during deposition process while contact depth was inversely decreased.

Figure 56 Graphical summarization on surface roughness, thickness, hardness, contact depth, and elastic modulus for Si wafer substrate and samples deposited with thin film at 80°C, 100°C, and 150°C.

CHAPTER V

CONCLUSIONS AND SUGGESTIONS

CONCLUSIONS AND SUGGESTIONS

This thesis has deal with an investigation on the physical mechanism behind the aluminum oxide thin films formed by Plasma enhance atomic layer deposition (PE-ALD) on silicon (1-0-0) substrates. The Alumina (Al_2O_3) thin films were grown using Trimethyl aluminum (TMA, Al $(CH_3)_3$) and O_2 as precursor reactants and argon as carrier gas. The study was compared the films properties deposited to 400 or 800 coating cycles and with or without plasma during deposition by varying substrate temperature from 80°C to 100°C and 150 °C. The evaluation methods involved several surface characterization techniques in terms of chemical and physical properties.

Surface roughness of samples deposited with thin film appeared to be similar to the virgin sample, i.e. smooth surface. Ra of all samples was ~0.18 nm and the root mean square roughness (Rq) of all samples was average to be ~0.2 nm. The number of coating cycles did not significantly impact to the surface roughness. Meanwhile deposition plasma obtained thicker and smoother films than without plasma. The films thickness strongly depended on plasma conditions and number of coating cycles, e.g. the thickness was 2.00 nm (400 cycles w/o plasma), 2.21 nm (400 cycles w/plasma), 2.41 nm (800 cycles w/o plasma) and 2.59nm (800 cycles w/plasma). AFM 3D images revealed the existing of sharp islands or particles clustering on sample surface deposited with plasma with sufficient film thickness. Increasing deposition temperature from 80ºC to 100ºC and 150ºC with plasma condition seems to reduce the film thickness. Generally, the increasing of temperature leads to a decline of growth rate, which mostly attributed to a decrease of the surface OH groups at higher temperatures. Moreover, upon the increasing of deposition temperature, the sharp islands or particles clustering seem to increase. The surface roughness of samples deposited with thin film increases with the deposition temperature. Rq of the samples deposited at 80ºC, 100ºC and 150ºC were 0.44, 0.36, and 0.51 nm respectively. The increasing of Rq value was attributed to the formation of sharp islands or particles clustering on sample surface as explained above.

The film thickness was also affected by the deposition temperature. As for 80ºC, 100ºC and 150ºC the thickness were 3.53 nm, 5.95 nm and 4.59 nm respectively.

Therefore, surface roughness and film thickness closely related to the deposition temperature. The surface morphology as observed by SEM (SE mode) with 40 KX magnifications displayed some particle clustering on the sample deposited at 150°C, confirming the AFM measurement.

Raman spectroscopy reported the existing of Al-O-Si system for the films deposited to 800 cycles with plasma at substrate temperature 80°. In this case, the Raman spectrum exhibited strong peak at ~498 cm^{-1}coincident with a spectrum of Diaspore which exhibited peaks at ~493 cm^{-1} and 2298 cm^{-1} [28]. Diaspore is one structure of aluminum oxide hydroxides and able to synthesize at temperature lower than 400°C [14]. However, the Raman spectrum of sample deposited without plasma exhibited a sharp band centered at ~520 cm^{-1} similar to the spectrum of Si wafer substrate. It points out that the film did not deposit on this sample.

Crystalline phase and film structure were characterized via XRD spectroscopy. The investigation samples were the samples deposited to 800 cycles with plasma and controlling temperature at 80°C, 100°C, and 150°C. XRD spectra exhibited the shapes, positions, and widths of the ~69° 2θ and the ~12° 2θ peaks and slight bump centered ~28° 2θ. The present of these features clearly indicates the formation of a crystalline AlOx-phase, e.g. diaspore, α - Al_2O_3 or γ- Al_2O_3. Note that diaspore can transformed to corundum (α-Al_2O_3) by annealing at temperature higher than 450°C with the pressure varying between 15000 to 30000 psi [32].

The chemical composition and the elements comprised to thin films were measured with XPS. The samples deposited with thin film to 800 cycles with plasma and controlling deposition temperature at 80°C, 100°C, and 150°C were extensively examined. However, aluminum element was not detected for all samples. It might be some contaminations remaining on sample surface after deposition obstructed the XPS performance, thus prohibit the X-rays to penetrate through the underneath thin films.

The morphology and composition of thin film was observed using TEM. BF images of samples deposited with thin film report that the films appeared to be amorphous. The technique could be able to define the interface between Al_2O_3 and SiO_2 and the thickness of Al_2O_3 film was estimated to be about 1.11 nm via HAADF profile maker. The EDX analysis was able to detect several chemical species, i.e. the film consisted of Cr, O, C, Si, Ca, Cu and Al.

Percentage of aluminum contents of the samples deposited at 80°C, 100°C, and 150°C were 0.33%, 0.43%, and 0.51% respectively. Based on this result, the percentage of aluminum content was increased with deposition temperature. Increasing of temperature during film growth affects to the film microstructure, for example increasing mobility of the species in the reaction. Note that only the subsequence thermal annealing could be able to convert the amorphous structure to the crystalline form.

Nano milling process is able to improve the cleanliness of the films by eliminating some contaminations covering the film layer. These contaminations prohibited the detection of actual deposition films. This process should be performed prior STEM scanning for increasing the efficiency of detection. After Nano milling, smooth surface area and cluster/rough surface area were examined and the aluminum contents were 0.66% and 1.54% respectively. The percentage of aluminum content increased when compared with the samples without Nano milling.

One could state the difference between TEM and XPS measurement on elements contents results. XPS was not able to detect Al element, suspecting of contamination or residue remaining on top of surface reducing the efficiency of XPS detection. As report above, Nano milling process was able to provide improvement and promotion the cleanliness of thin film surface and it should apply prior any thin film characterization. For example, the elements comprised of deposited film can subsequently be measured by SEM using EDS mode. The EDS spectrum of samples deposited with thin film at 150° displayed Al peak.

Mechanical properties, e.g. hardness (H), Elastic reduced Modulus (Er), and contact depth (hc) were measured by Nano indentation using Berkovich tip. For deposition at controlling temperature 80°C, the samples deposited to 800 cycles with plasma was harder and their elastic modulus higher than without plasma. Their hardness and elastic modulus also better than samples deposited to400 cycles for both with and without plasma. Note that using 70 μN indentation forces, contact depths for all deposited samples did not change significantly in comparison with Si wafer substrate. Further study was focused on temperature effects, i.e. samples were deposited at 80°C, 100°C, and 150°C by controlling deposition cycle to 800 and using plasma during deposition. The mechanical properties were significantly correlated to the deposition temperature. Using 100 μN indentation forces, sample deposited at 150°C was the best conditions in term of hardness, elastic reduced modulus, and contact depth.

FURTHER WORK

The technique of synthesizing Al_2O_3 thin film by PE-ALD as reported by this thesis can be applied to many thin film technology. On one hand, the excellence properties of Al_2O_3 material allow them to be used in various applications. On the other hand, PE-ALD technique is able to grow films to the angstrom level thickness at relatively low temperature. Based on this thesis, the AlOx phase was initially formed at the temperature as low as 80°C. Although, this phase normally transform to alumina phase (α-Al_2O_3) at temperature higher than 400°C, but we can solve this problem by subsequently annealing at high temperature. Post annealing induces modification of film composition, reduction of pin-holes, and increasing of grain sizes. Annealing also influences the crystallinity and the mechanical properties of materials. For advance application, we can apply Al_2O_3 thin films for photo-catalytic technology in which TiO_2 was employed. In this case Al_2O_3 thin film may be deposited on the samples surface after the completion of TiO_2 coating, leading to using both films with extreme benefit. Such that Al_2O_3 is electric conduction depends primarily on impurities, which act as acceptors and TiO_2 as donors. Hence, both materials can be balancing between electric and ionic contribution, thus applicable for many function as require.

BIBLOGRAPHY

BIBLOGRAPHY

1. Richard W. Johnson, Adam Hultqvist, and Stacey F. Bent. A brief review of Atomic layer deposition. Fundamentals to Applications. 2015;17(5):236–246.
2. Steven M. George. Atomic Layer Deposition: An Overview. Journal of Chemical Reviews. 2010;110(1):111-131.
3. Erwin Kessels; et al. Opportunities for Plasma-Assisted Atomic layer Deposition. Journal of ECS Transactions. 2007;3(15):183-190.
4. Harald B. Profijt, Stephen E. Potts, M. C. M. Richard van de Sanden, and W. M. M Ervin Kessels. Plasma- Assisted Atomic Layer Deposition: Basics, Opportunities, and Challenges. Journal of Vacuum Science & Technology A. 2011;29(5):050801-1 - 050801-26.
5. Rupesh Kumar, Vishnu Prabhakar, and Jasmeen Saini. Alumina. International Journal of Current Engineering and Technology. 2013;3(5):1676 -1685.
6. M.L. Guzman-Castillo, X. Bokhimi, A. Rodrıguez-Hernandez, A. Toledo-Antonio, F.Hern_andez-Beltran, and J.J. Fripiat L. The surface energy of quasi-amorphous γ-alumina calculated from the temperature of the $\gamma \longrightarrow \alpha$ transition. Journal of Non-Crystalline Solids. 2003;329:53–56.
7. Ibrahima Sory Cissé, Jiwen Ge. Determination of Bauxite's phases by the bomb digest method at Kamsar laboratory ISO 9002 (Guinea). Journal of American Science. 2010;6(6):139 - 145.
8. Karen Davis. Material Review: Alumina (Al_2O_3). School of Doctoral Studies (European Union) Journal. 2010:109-114.
9. Kaiyun Jiang. Al_2O_3 Thin Films: Relation between Structural Evolutions, Mechanical Properties and Stability. Materials Chemistry Dissertation Shaker Verlag. Aachen.2011:9.
10. Yuilun Wu. Deposition of alumina oxide by Evaporative coating atmospheric pressure (ECAP). University of Illinois at Urbana-Champaign. 2013:2.
11. Takashi Shirai, Hideo Watanabe, Masayoshi Fuji and Minoru Takahashi. Structural Properties and Surface Characteristics on Aluminum Oxide Powders. Ceramics Research Laboratory, Nagoya Institute of Technology. 2009;9:23-31.

12. Igor Levin, and David Brandon. Metastable Alumina Polymorphs: Crystal Structures and Transition Sequences. Journal of the American Ceramic Society.1998;81(8):1995 – 2012.

13. Milton Ohring. Material Science of thin film, 2nd edition. Acamimic Press. 2003:277-618.

14. Ferando J. Aponte Rivera. Nucleation, Growth, and Electrical Characterization of Al_2O_3 Thin films grown by Atomic layer Deposition. Department of Physics. University of Pureto Rico- Rio Piedras Campus, San Juan, Puerto Rico. 2015:12.

15. Sakari Ruppi. Deposition microstructure and properties of texture-controlled CVD α - Al_2O_3 coatings. International Journal of Refractory Metals and Hard Materials.2005;23:306-316.

16. Vale´rie Meille. Review on methods to deposit catalysts on structured surfaces. Applied Catalysis A: General 315. 2006:1–17.

17. Philip Anu. Preparation and Characterization of High-k Aluminum Oxide Thin Films by Atomic Layer Deposition for Gate Dielectric Applications. Cochin University of Science and technology. Department of Instrumentation Cochin University of Science and Technology. Kerala, India.2011.

18. Ville Miikkulainen, Markku Leskela, Mikko Ritala, and Riikka L. Crystallinity of inorganic films grown by atomic layer deposition: Overview and general trends. Journal of Applied Physics. 2013;113(2):021301-1- 021301-101.

19. S. Gieraltowska; et al. Properties and characterization of ALD grown dielectric oxides for MIS structures. Acta Physica Polonica.2011:119333-336

20. Kurt W. Kolasnski. Surface science: Fundation of catalysis and nanoscience 2nd edition. Department of chemistry, West Chester University West Chester. Surface science.2008:127-135.

21 Johanna Rosen, Jochen M. Schneider, and Karin Larsson. Thin Film Growth Related Adsorption Study of Al and O Ions on an α- Al_2O_3 Surface. The Journal of Physical Chemistry B. 2004;108(50):9320-19324.

22. M. Leskela and M. Ritala. Atomic layer deposition (ALD) from precursor to thin film structure. Thin film. 2002;409:138-146.

23. A. Dechana, P. Thamboon, and D. Boonyawan. Microwave remote plasma Enhanced –atomic layer deposition system with multicusp confinement chamber. Review Of Scientific Instruments.85:2014:103510-1 - 103510-7.

24. Robert A. Wilson and Heather A. Bullen. Basic Theory Atomic Force Microscopy (AFM). Department of Chemistry, Northern Kentucky University, Highland Heights, KY 41099.2006.

25. M. Raposo, Q. Ferreira, and P.A. Ribeiro. A Guide for Atomic Force Microscopy Analysis of Soft- Condensed Matter. Modern Research and Educational Topics in Microscopy. FORMATEX Microscopy series N° 3.2: 2007:758-769.

26. V. Cimalla; et al. Densification of Thin Aluminum Oxide Films by Thermal Treatments. Materials Sciences and Applications.2014;5:628-638.

27. Jorg Haeberle; et al. Ellipsometry and XPS comparative studies of thermal and plasma enhanced atomic layer deposited Al_2O_3-films. Beilstein Journal of Nanotechnology.2013;4:32–742.

28. J. Zhang Jian, Li Hai-Tao, GUO Jun-Hong, HU Fang-Ren.Raman Scattering Modification Induced by Structural Change in Alumina Polymorph. Chinese physics Letter. 2015;32(12):26801-4

29. Erik Wallin; et al. Synthesis of α -Al_2O_3 thin films using reactive high power impulse magnetron sputtering. Europhysics letters. 2008;(82):36002.

30. Rajesh Katamreddy; et al. ALD and characterization of alumina oxide deposition on Si (100) using tris (diethlylamino) Aluminum and water. Journal of The Electrochemical Society. 2006;153:701-706.

31. B. K. Tanner; T. P. A. Hase; T. A. Lafford; and M. S. Goorsky. Grazing Incidence In – Plane X-Ray Diffraction in Laboratory. International Centre for Diffraction Data Advances in X-ray Analysis. 2004;47:309-341

32. Teng-Shih Shih and Zin-Bou Liu.Thermally-Formed Oxide on Aluminum and Magnesium. Materials Transactions. 2006;47(5):1347-1353.

33. Oliver, Warren C, and Georges M. Pharr. Measurement of hardness and elastic modulus by instrumented indentation: Advances in understanding and refinements to methodology. Journal of materials research.2004;19(1):4-5.

34. Xuwen Liu; et al.On the reliability of nanoindentation hardness of Al_2O_3 films grown on Si-wafer by atomic layer deposition. Journal of Vacuum Science & Technology A.2014; 32(1):01A116-1- 01A116-6.

35. Jorg Haeberle; et al. Ellipsometry and XPS comparative studies of thermal and plasma enhanced atomic layer deposited Al_2O_3-films. Beilstein Journal of Nanotechnology. 2013;4:732–742.

36. O Hahtela; et al. Atomic layer deposited alumina (Al_2O_3) thin films on a high-Q Mechanical silicon oscillator. Journal of Micromechanics and Micro engineering. 2007;17:737-742.

37. M. Smietana;et al.Capability for Fine Tuning of the Refractive Index Sensing Properties of Long-Period Gratings by Atomic Layer Deposited Al_2O_3 Overlays. Journal of Sensors. 2013;13:16372-16383.

38. S. Lee; and H. Jeon. Characteristics of an Al_2O_3 Thin Film Deposited by a Plasma Enhanced Atomic Layer Deposition Method Using N_2O Plasma. Electronic Materials Letters.2007;3(1):17-21.

39. K Ali, CY. Kim, and KH. Choi. Characterization of Al_2O_3 thin films fabricated through atomic layer deposition on polymeric substrates. Journal of Materials Science: Materials in Electronics. 2014;25:1922–1932.

40. M. D. Groner; et al. Low-Temperature Al_2O_3 Atomic Layer Deposition. Journal Chemistry of Materials.2004;16(4):639-645.

41 Yude Shen; et al. Excellent insulating behavior Al_2O_3 thin films grown by atomic layer deposition efficiently at room temperature. Optoelectronics and advanced materials–rapid communications.2012;6(5-6):618-622.

42 Wang ZY; et al. The impact of thickness and thermal annealing on refractive index for aluminum oxide thin films deposited by atomic layer deposition. Nanoscale Research Letters.2015;10(46).

VITA

VITA

Name	Miss Paramaporn Jitsopakul
Date of birth	3 August 1980
Present address	9 / 449 Moo. 14 Mooban Ratchapruek 7, T. Klong Neung A. Klong Luang, Prathumthani, Thailand 12120
E-mail address	au_1463@hotmail.com
Mobile	086-808-9736

EDUCATION

1999	High school diploma M.6 (Math-Science), Benjama –Maharat From School, Ubonratchathani.
2003	Bachelor Degree Science of Biotechnology, From Mahasarakham University.
2016	Master Degree of Material Science, From Srinakharinwirote University.